



Similarity-Based Nonlinear Settlement Predictions of Circular Surface Footings on Clay

Abigail H. Bateman¹; Jamie J. Crispin, Ph.D.²; Dimitris Karamitros, Ph.D.³; and George E. Mylonakis, Ph.D., P.E., M.ASCE⁴

Abstract: The similarity method, employed to obtain nonlinear settlement predictions in undrained conditions for rigid circular footings on deep clay deposits, was introduced more than 70 years ago. This approach is based on the premise that the pressure–settlement curve of the footing and a stress–strain curve from a characteristic point in the soil can be linearly scaled to collapse into a single master curve. The method has been extended to predict deflections of axially and laterally loaded piles and is widely used in the offshore industry. Despite the theoretical and practical appeal of the method as well as its wide application in a range of geotechnical problems, limited investigation and validation exists in the literature. In this work existing classical similarity methods are reviewed, including a Boussinesq solution for elastic soil and the mobilizable strength design (MSD) method. The similarity factors derived from these methods are compared with those obtained from a novel nonlinear cone model solution, and the resulting expressions are evaluated against rigorous numerical analyses undertaken by the authors in FLAC. These are based on two different nonlinear constitutive models (hyperbolic and tanh) calibrated against triaxial tests from three clay deposits. Two alternative families of similarity methods are also compared with classical similarity, namely, a two-part similarity technique (based on separate scaling factors for elastic and plastic strains) and a stiffness similarity approach (based on secant stiffness degradation). Finally, three field test results are evaluated as case studies to demonstrate the applicability of the method in real-life problems. It is concluded that similarity approaches offer a rational yet approximate tool for nonlinear settlement analysis of footings. DOI: 10.1061/JGGEFK.GTENG-12641. This work is made available under the terms of the Creative Commons Attribution 4.0 International license, https://creativecommons.org/licenses/by/4.0/.

Author keywords: Surface footings; Settlement; Nonlinear analysis; Soil-structure interaction; Similarity.

Introduction

Improved understanding of the nonlinear pressure–settlement response of surface footings on clay would enable more efficient design to prevent excessive settlements. Simple analytical solutions are available to determine both the fully elastic initial slope of the pressure–settlement curve as well as the perfectly plastic failure load [e.g., Skempton (1951) and Brinch Hansen (1970) and as discussed in a recent summary by Salgado (2022)]. Of particular interest is the elastic solution for the stiffness of a rigid footing on the surface of an elastic half-space established by Boussinesq (1885) (Poulos and Davis 1974; Davies and Selvadurai 1996). Some empirical solutions for the pressure–settlement response of surface footings (e.g., Jardine et al. 1995; Lehane 2003; Agaiby and Ahmed 2022) are available in the literature, as well as some numerical

¹Ph.D. Student, Dept. of Civil Engineering, Univ. of Bristol, Bristol BS8 1TR, UK (corresponding author). ORCID: https://orcid.org/0000-0003-3454-1756. Email: a.bateman@bristol.ac.uk

²Lecturer, Dept. of Civil, Maritime and Environmental Engineering, Univ. of Southampton, Southampton SO16 7PN, UK; formerly, Postdoctoral Research Assistant, Dept. of Engineering Science, Univ. of Oxford, Oxford OX1 3PH, UK. ORCID: https://orcid.org/0000-0003-3074-8493

³Senior Lecturer, Dept. of Civil Engineering, Univ. of Bristol, Bristol BS8 1TR, UK. ORCID: https://orcid.org/0000-0002-3185-7838

⁴Professor, Dept. of Civil Infrastructure and Environmental Engineering, Khalifa Univ., Abu Dhabi, UAE; University Chair in Geotechnics and Soil-Structure Interaction, Dept. of Civil Engineering, Univ. of Bristol, Bristol BS8 1TR, UK. ORCID: https://orcid.org/0000-0002-8455-8946

Note. This manuscript was submitted on January 9, 2024; approved on December 4, 2024; published online on April 16, 2025. Discussion period open until September 16, 2025; separate discussions must be submitted for individual papers. This paper is part of the *Journal of Geotechnical and Geoenvironmental Engineering*, © ASCE, ISSN 1090-0241.

solutions (e.g., Osman and Bolton 2005; Ghosh Dastider et al. 2021). However, these solutions are limited to specific soil–footing configurations and may require site-specific studies that are costly and time-consuming to undertake.

Alternatively, nonlinear pressure-settlement curves can be determined using theoretical models such as the cavity expansion theory introduced by Bishop et al. (1945) for metals and later extended by Gibson (1950) to clay soils [also employed for penetration resistances in sand (e.g., Salgado et al. 1997; Salgado and Prezzi 2007)]. This method has been employed by McMahon et al. (2013) using an energy approach to estimate a nonlinear pressure settlement curve for a surface footing on an elastic-perfectly plastic half space and has been further extended by McMahon et al. (2014) to incorporate a nonlinear soil constitutive model. Alternatively, Klar and Osman (2008) developed a nonlinear pressure–settlement curve by combining an elastic and an elastoplastic mobilizable strength design (MSD) solution using an energy method to weigh the contributions of the two mechanisms. However, despite the frequency with which this problem is encountered in routine engineering practice and its importance in settlement estimation, limited analytical solutions are available to determine the full nonlinear pressure-settlement curve.

A simple approach to obtain a nonlinear pressure–settlement curve for footings was introduced by Skempton (1951), who suggested that a pair of linear scaling factors for stresses and strains can be used to transform a stress–strain curve directly into a pressure–settlement curve and vice versa. This approach (which is referred to in the ensuing as *classical similarity*) is based on the premise that there is similarity in shape between a stress–strain curve from a laboratory test and the foundation pressure–settlement curve (Fig. 1). In the realm of this approach, the nonlinear pressure–settlement curve of a vertically loaded footing can be obtained directly from

ASCE 04025050-1 J. Geotech. Geoenviron. Eng.

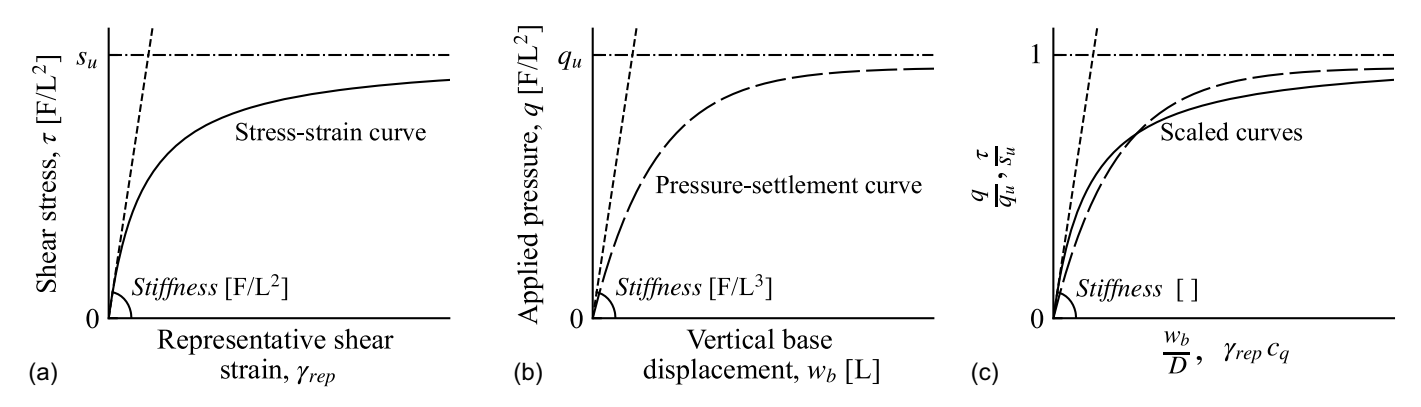


Fig. 1. (a) Idealized stress—strain curve from an element test of a representative soil sample; (b) idealized pressure—settlement curve of a foundation; and (c) normalized and transformed curves seeking similarity.

a routine laboratory test using two linear transformation factors, one scaling each axis.

Classical similarity has been employed for surface footings by Elhakim (2005), Osman et al. (2007), and Agaiby and Ahmed (2022). An analogous similarity has been utilized to obtain t–z curves for axially loaded piles (e.g., Seed and Reese 1957; Fu et al. 2020; Bateman et al. 2022a), as well as p–y curves for laterally loaded piles (e.g., McClelland and Focht 1956; Matlock 1970; Kagawa and Kraft 1981; Bransby 1999; Reese and Van Impe 2011) and associated m– θ curves (e.g., Fu et al. 2020; Bateman et al. 2023). Although the cost and time benefits from this approach can hardly be overstated, there is no guarantee that such similarity exists for each case considered, and the resulting predictions should be considered as approximate.

For the classical similarity method [as originally suggested by Skempton (1951)] to be usable in routine design of vertically loaded circular footings, suitable values of the scaling factors must be determined. Furthermore, the accuracy and limits of the similarity approach should be established. This could be done through either numerical modeling (e.g., finite-element analysis), or field and laboratory testing where both stress–strain and pressure–settlement curves are obtained.

Alternative Similarity Approaches

The classical similarity approach has also been extended using a two-part similarity method that consists of individual scaling factors applied individually on the elastic and plastic portions of the curve. Previously, this approach has been employed for t-z curves for axially loaded piles by Fu et al. (2020); p-y curves by Jeanjean et al. (2017), Zhang and Andersen (2017, 2019), and Fu et al. (2020); and base curves for laterally loaded piles by Fu et al. (2020) and Lai et al. (2020). This approach has also been used implicitly by Jakub (1977), who assumed that a secant stiffness–stress curve can be given in the same form as a secant stiffness–load curve for a strip footing under dynamic horizontal and moment loading.

Additionally, Atkinson (2000) suggested a stiffness similarity approach based on the shapes of the secant stiffness–strain $(G-\gamma)$ curve from a triaxial soil test and a secant stiffness–settlement $(K-w_b)$ curve of a footing. Employing similar arguments to those of Skempton, Atkinson (2000) proposed a linear transformation factor to relate between these two curves.

This Paper

Despite the theoretical importance and practical appeal of these simplified methods, their existence for a long period of time and their applicability in a wide range of geotechnical problems, limited validation has been carried out, and some authors have even questioned some of the fundamental assumptions (Burland et al. 1966; Randolph and Wroth 1978). More importantly, there is currently limited understanding of the underlying principles and the way these methods relate to and differ from one another.

Motivated by this gap in knowledge, this paper investigates the similarity proposal and its variants as applied to obtain a pressure–settlement curve of a vertically loaded circular surface footing on clay from a corresponding stress–strain curve of a soil element test. This involves (1) a review of existing methods related to the similarity approach, (2) reformulating these solutions into a consistent framework, and (3) developing and validating the novel expressions for the required transformation factors using both analytical and numerical methods. Specifically, this paper undertakes the following:

- The classical similarity proposal by Skempton (1951) to directly relate stress-strain and pressure-settlement curves is first reviewed. To this end, two related methods, an elastic stiffness approach based on the Boussinesq solution and the MSD method, are reformulated in a consistent framework to derive linear-transformation factors.
- A novel nonlinear solution using a cone model for pressuresettlement curves is derived, inspired by related elastic solutions to dynamic footing problems. This is used to derive lineartransformation factors for specific nonlinear soil constitutive models.
- The methods are compared and validated by means of rigorous numerical solutions in the finite difference software FLAC 2D version 7.0. Two different nonlinear soil constitutive models are used, calibrated against three different types of clay.
- The alternative two-part similarity approach is applied to the vertically loaded foundation problem for the first time. An analytical solution, in conjunction with further numerical results, is employed to derive novel linear-transformation factors for this method.
- The stiffness similarity approach proposed by Atkinson (2000) to directly relate secant stiffness—strain with secant stiffness—settlement curves is reviewed. A novel closed-form expression for the similarity factor for an elastic-perfectly plastic material is derived and compared with the original values from Atkinson (2000) and those obtained from the FLAC results.
- The three similarity methods are compared, and the appropriate choice of linear transformation factors is discussed for different loading ranges. These factors are applied to predict the pressure settlement curve for three case study examples and demonstrate the use and limitations of these approaches.

Classical Similarity

The classical similarity approach is demonstrated in Fig. 1. Employing this method requires the selection of two linear transformation factors, one for each axis. Given the two curves are similar in shape, the linear transformation factor of the y-axis can be obtained by comparing the ultimate capacity of each curve, which naturally bounds both curves between zero and one. Specifically, the pressure–settlement curve approaches the ultimate capacity of the footing, q_u and the stress–strain curve approaches the undrained soil shear strength, s_u . It is well-known that the ultimate capacity of a footing in clay can be given by a dimensionless bearing capacity factor, N_c , multiplied by s_u . Therefore, the scaling factor on the y-axis is simply N_c (values for which are discussed later).

Secondly, the x-axis of the pressure–settlement curve should be normalized by a characteristic dimension, with the aim of collapsing the two curves into a single master curve. This characteristic dimension is selected here to be proportional to the footing diameter, D, with a dimensionless proportionality constant, defined here as a linear transformation factor, c_q . Therefore, the linear transformation of the x-axis can be expressed by

$$\gamma_{\text{rep}} = \frac{w_b}{c_q D} \tag{1a}$$

where γ_{rep} = representative average shear strain of the soil under the footing; and w_b = footing settlement.

Inverting this equation gives the footing settlement, w_b , obtained by scaling the representative strain by the characteristic dimension c_aD as follows:

$$w_b = \gamma_{\rm rep} c_q D \tag{1b}$$

The key idea behind this approach is that $\gamma_{\rm rep}$ can be established from a pertinent soil element test under the same level of normalized stress (i.e., $\tau_{\rm rep}=q/N_c$). Therefore, after appropriate N_c and c_q values have been selected, the following simple steps should be followed to employ this approach in design:

- 1. Divide q, the pressure applied to the foundation, by N_c to get the corresponding $\tau_{\rm rep}$, the shear stress on the representative soil sample.
- 2. Use a representative soil element test (or an assumed constitutive model) to obtain $\gamma_{\rm rep}$, the strain in the representative soil sample at $\tau_{\rm rep}$.
- 3. Use Eq. (1b) to obtain w_b , the foundation displacement, under the applied pressure.

The selection of the footing diameter to normalize settlement is an arbitrary decision, and alternative selections (e.g., the footing radius) can be equally valid and merely scale the transformation factor c_q . Furthermore, Eq. (1) is defined with a representative shear strain that is obtained from a soil element test undertaken on a representative soil sample. To employ the similarity approach, the location of a representative soil sample under the footing must be identified and a suitable soil element test (e.g., triaxial compression) selected. Using finite-element analysis (FEA), Osman and Bolton (2005) suggested that this representative sample should be taken from a depth of 0.3D beneath the center of the footing. However, a greater understanding of the relevance of the location of the representative soil sample is required before this approach can be adopted in design.

Additionally, the stress–strain curve of the representative soil sample may depend on which type and shear mode of element test is chosen. Within the original similarity proposal, Skempton (1951) suggested an undrained compression (triaxial) test would be suitable. Because the choice of sample location and test type are outside

the scope of this work, an idealized isotropic homogeneous clay is considered. This means that any element test will produce identical results for a test in any location.

The value of N_c at the surface has been considered by many authors and is dependent on the foundation shape and roughness. Shield (1955) and Eason and Shield (1960) calculated N_c for a circular rigid footing to be 5.69 and 6.05 for a perfectly smooth and rough footing conditions, respectively. Alternative N_c values for footings are available (e.g., Ishlinsky 1944; Skempton 1951; Meyerhof 1951; Cox et al. 1961; Brinch Hansen 1970; Tani and Craig 1995; Salgado et al. 2004; Gourvenec et al. 2006). These solutions vary between $5.58 < N_c < 6.23$. However, the solutions by Shield (1955) and Eason and Shield (1960) are both lower and upper bounds and have subsequently been verified by Houlsby and Wroth (1984) as essentially exact values (Martin and Randolph 2001).

Similarly, some solutions for c_q in various forms can be found in the literature. Notably, the MSD method used by Osman and Bolton (2005) is a form of classical similarity. These authors derived a coefficient M_c (the reciprocal of the linear transformation factor) as the average shear strain within an assumed displacement mechanism. Any M_c value can be converted to a c_a value that follows the definition used in Eq. (1) (discussed subsequently). In fact, any method that obtains a pressure-settlement curve from a soil stress-strain curve, including numerical analysis and experimental data, can be reformulated as a c_q value. Therefore, the methods to obtain c_q can be broadly split into two main categories: (1) those that obtain c_a directly, without employing a pressure–settlement curve; and (2) those that derive c_q by comparing a pressure-settlement curve with the respective stress-strain curve. Although a single c_q value would suggest perfect similarity exists, for most cases, c_q will vary with applied load as well as soil properties.

Elastic Stiffness Approach

Skempton (1951) suggested a method to analytically obtain c_q for a circular surface footing by assuming an elastic half-space and matching the stiffnesses of the two curves. To this end, the linear-elastic soil constitutive model can be expressed in normalized form as follows:

$$\frac{\tau}{s_u} = \left(\frac{G}{s_u}\right)\gamma\tag{2}$$

where τ and γ = applied shear stress and strain, respectively; G = soil shear modulus; and s_u = soil undrained shear strength.

The elastic settlement of a rigid circular footing can be established using the Boussinesq solution (Boussinesq 1885; Poulos and Davis 1974; Davies and Selvadurai 1996). The resulting pressure—displacement relationship can be normalized by the ultimate bearing pressure $q_u \ (= N_c s_u$ for undrained conditions), to yield the following dimensionless equation:

$$\frac{q}{q_u} = \frac{K_i w_b}{q_u} = \frac{8}{\pi (1 - \nu_s)} \left(\frac{G}{N_c s_u}\right) \frac{w_b}{D} \tag{3}$$

where q= mean pressure acting on the soil-footing interface; $q_u=$ corresponding ultimate bearing pressure; $K_i=$ elastic stiffness of the footing; $\nu_s=$ Poisson's ratio of the soil; and $N_c=$ bearing capacity factor.

The aforementioned solution was developed assuming a smooth footing–soil interface. An alternative solution is available for a rough footing–soil interface (Spence 1968); however, for undrained conditions, this is equivalent to Eq. (3), subject to the selection of appropriate N_c values.

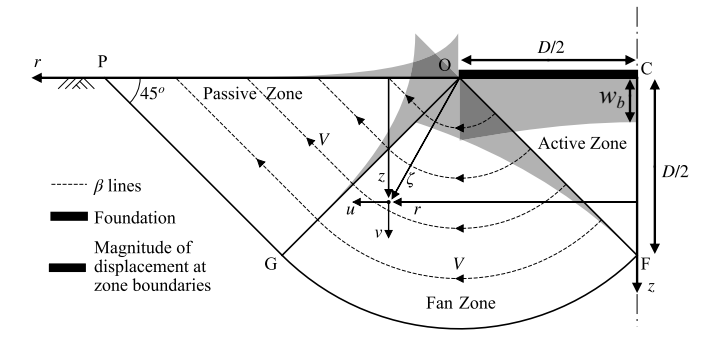


Fig. 2. Illustration of the assumed plastic deformation mechanism developed by Osman and Bolton (2005) for circular surface footings in cylindrical coordinates.

For soft soil, the left-hand sides of Eqs. (2) and (3) are naturally bounded between zero and one. Therefore, equating the right-hand side of these equations and introducing c_q in the form of Eq. (1) yields the following linear-transformation factor:

$$c_{q} = \frac{\pi}{8} (1 - \nu_{s}) N_{c} \tag{4}$$

which, remarkably, is independent of G and s_u .

The essentially exact N_c values for smooth and rough circular footings produced by Shield (1955) and Eason and Shield (1960), i.e., 5.69 and 6.05, and considering $\nu_s=0.5$, result in a c_q of 1.12 and 1.19, respectively. This value is roughly equivalent to the factor of 2 (applied to normal strain instead of shear strain) obtained by Skempton (1951), dependent on the selected N_c . The full range of available N_c mentioned in this paper result in c_q values of $1.10 < c_q < 1.22$.

Mobilizable Strength Design Method (Osman and Bolton 2005)

The MSD method was introduced by Bolton and Powrie (1988) for earth pressures and has primarily been used in the design of deep excavations (e.g., Osman and Bolton 2004). The method has been extended by Osman and Bolton (2005) to obtain c_q values for vertically loaded circular footings. The resulting values have been compared against numerical and field data (Osman et al. 2007).

Osman and Bolton (2005) employed a displacement field where the outer boundaries are defined using a Prandtl-like failure mechanism modified for axisymmetric loading. Within the boundaries, three regions are defined: the active, fan, and passive zones, in which the displacement field was chosen such that shear strains and displacements remain compatible (Fig. 2). Either side of the fan zone (boundaries OF and OG in Fig. 2) vertical and radial

displacements are equal in magnitude and direction. Beyond the mechanism boundaries (boundary FGP in Fig. 2) the soil is assumed perfectly rigid. Finally, as the loading conditions are undrained, no volume change is assumed. The soil strains are therefore constrained by the following equation:

$$\varepsilon_r + \varepsilon_\theta + \varepsilon_z = -\frac{\partial u}{\partial r} - \frac{u}{r} - \frac{\partial v}{\partial z} = 0$$
 (5)

where u and v = radial and vertical displacements, respectively; and $\varepsilon_r = -\partial u/\partial r$, $\varepsilon_\theta = -u/r$, and $\varepsilon_z = -\partial v/\partial z$ are the normal strains in the cylindrical coordinate system defined by r, θ , and z as illustrated in Fig. 2, respectively. Additionally, shear strains in axisymmetric conditions are $\gamma_{r\theta} = 0$, $\gamma_{\theta z} = 0$ and $\gamma_{zr} = -(\partial v/\partial r + \partial u/\partial z)$.

Regarding the selection of the displacement mechanism, Osman and Bolton (2005) assumed the variation of vertical displacements along the center line (CF in Fig. 2) can be given by a quadratic polynomial. They also assumed that within the active zone, the vertical displacements are independent of radial distance. Thus, by considering Eq. (5) and applying boundary conditions (u=0 at r=0; $v=\delta$ at r=0 and z=0; and u=v along boundary OF), u and v can be derived as given in Table 1. These assumptions correspond to a smooth footing (i.e., there are nonzero radial soil displacements at the footing—soil interface). Also, contrary to Prandtl's mechanism, soil is not at a state of failure so the displacement field is continuous and displacements are zero along the outer boundary PGF in Fig. 2.

Following the assumption that the radial and vertical displacements on either side of each zone boundary are equal, the u and v in the fan and passive zones can be calculated, also given in Table 1. Note that, to ensure zero volume change, the total displacement in the fan and passive zones $(\sqrt{u^2+v^2})$ must decay proportional to 1/r (Osman and Bolton 2005), which is slower than predicted by the Boussinesq solution.

The radial and vertical displacements in Table 1 can be converted into normal and shear strains, which are employed to calculate the principal strains ε_1 , ε_2 , and ε_3 . The resulting mobilized engineering shear strain ($\varepsilon_1 - \varepsilon_3$) can then be averaged over the mechanism and set equal to the representative shear strain $\gamma_{\rm rep}$ in Eq. (1) as follows (Osman and Bolton 2005):

$$\gamma_{\text{rep}} = \frac{\int_{\text{vol}} |\varepsilon_1 - \varepsilon_3| d\text{vol}}{\int_{\text{vol}} d\text{vol}} = M_c \frac{w_b}{D} = \frac{w_b}{c_q D}$$
 (6)

This approach yields a single value of $c_q=0.74$ [equivalent to $M_c=1/c_q=1.35$ in the notation of Osman and Bolton (2005)] that is independent of the footing dimension and developing settlement. This value implies a smaller characteristic dimension (lower c_q) than the elasticity solution of Eq. (4), which is associated with the confined area of plastic strain concentration, compared

Table 1. Radial, u, and vertical, v, displacements in each zone for surface

Zone	Radial displacement, u	Vertical displacement, v			
Active	$w_b \left(\frac{2r}{D} - \frac{4rz}{D^2}\right)$	$w_b \left(\frac{4z^2}{D^2} - \frac{4z}{D} + 1 \right)$			
Fan	$2w_b\left(\frac{z}{r}\right)\left(\frac{D}{\zeta}\right)\left(\frac{\sqrt{2}}{2}-\frac{\zeta}{D}\right)^3$	$-2w_b\left(\frac{z}{r}\right)\left(\frac{r}{D}-\frac{1}{2}\right)\left(\frac{D}{\zeta}\right)\left(\frac{\sqrt{2}}{2}-\frac{\zeta}{D}\right)^3$			
Passive	$\frac{w_b}{2} \left(\frac{D}{r} \right) \left(\frac{3}{2} - \frac{r}{D} - \frac{z}{D} \right)^3$	$-\frac{w_b}{2} \left(\frac{D}{r}\right) \left(\frac{3}{2} - \frac{r}{D} - \frac{z}{D}\right)^3$			

Note: $\zeta = \text{polar distance from the center of the fan given by } \zeta/D = \sqrt{(r/D - 1/2)^2 + (z/D)^2}$ (Fig. 2).

with the strain distribution across a wider area in the elastic solution. Thus, it is thought that this value may pertain better to situations of higher load levels, where significant plastic deformation has taken place.

The MSD method has the advantage that it calculates c_q directly and does not depend on the selection of a soil constitutive model and the level of applied load. However, it is dependent on the geometry (size) of the chosen deformation mechanism, which indirectly relates to the concentration of high strains near the footing.

Cone Model

Cone models have been widely used in footing displacement calculations. Considering a surface footing of diameter D, and area A_b , loaded by a vertical traction q, vertical stress attenuates with depth based on a selected cone opening line f(z), assumed here to be linearly varying with gradient $1/m_{\rm cone}$, as shown in Fig. 3. Original applications often refer to this approach as the 2:1 method and set $m_{\rm cone}$ between one and two (Bowles 1997). Wolf and Deeks (2004) also provided static solutions using the cone model for lateral and rocking modes. This paper applies a cone model to determine novel solutions for the nonlinear vertical pressure–settlement curves of footings from which c_q values are derived.

Following the cone model logic, it is assumed that the vertical normal strain, ε , can be integrated over the depth, z, to furnish the settlement of the footing, w_b

$$w_b = \int_0^\infty \varepsilon(z)dz \tag{7}$$

The vertical strain, ε , can be written as a function of the normalized deviatoric stress, $g(\sigma_q/2s_u)$, by introducing a pertinent soil constitutive model in flexibility form. The normalized deviatoric stress within the soil, $\sigma_q(z)/2s_u$, is taken as equal to the normalized vertical stress at depth $q_z(z)/q_u$ due to the footing load. This is arguably a similarity assumption itself. Additionally, vertical equilibrium is assumed between horizontal layers of the cone itself and the stress at depth, z, which is considered to be uniform over the area $A_z(z)$. This can be written

$$q_z(z)A_z(z) = qA_b \tag{8}$$

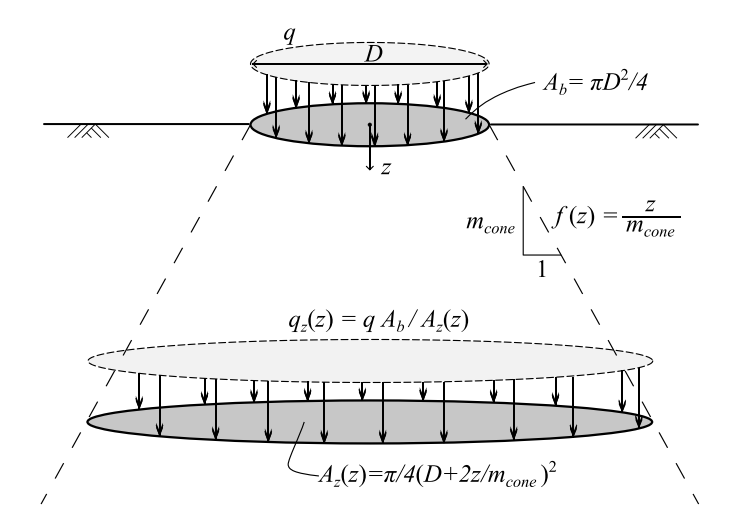


Fig. 3. Application of the cone model to obtain pressure–settlement curves.

where $A_z(z)$ depends on the chosen $m_{\rm cone}$. This key assumption implies that tractions developing along the cone boundary are horizontal (or zero). It also means $m_{\rm cone}$ must have a dependency on the Poisson's ratio of the soil in order to match the overall elastic stiffness of the foundation. Therefore, by using a constant $m_{\rm cone}$ value over the full range of stresses, it is effectively assumed that the Poisson's ratio of the soil remains constant.

Based on these assumptions, the vertical normal strain is given by

$$\varepsilon = g\left(\frac{\sigma_q}{2s_u}\right) = g\left(\frac{q_z(z)}{q_u}\right) = g\left(\frac{q}{q_u}\left(\frac{A_b}{A_z(z)}\right)\right) \tag{9}$$

Firstly, assuming the soil is described using a linear-elastic soil constitutive model [Eq. (2)] $[\varepsilon = \gamma/(1 + \nu_s), \ \sigma_q = 2\tau(z)]$, then

$$\varepsilon = \frac{\sigma_q}{2G(1+\nu_s)} = \frac{s_u}{G(1+\nu_s)} \left(\frac{q_z(z)}{q_u}\right) \tag{10}$$

Substituting this function into Eq. (7) and evaluating the integral using the depth-varying area $A_z(z)$ shown in Fig. 3 yields the elastic settlement of the footing as a function of the applied stress as follows:

$$\frac{w_b}{D} = \frac{m_{\text{cone}}}{2(1+\nu_s)} \left(\frac{s_u}{G}\right) \left(\frac{q}{q_u}\right) \tag{11}$$

By employing the concept of similarity and comparing this equation with the normalized shear stress-strain curve [Eq. (2)], c_q simplifies to

$$c_q = \frac{m_{\text{cone}}}{2(1 + \nu_s)} \tag{12}$$

which is again independent of the footing dimension and the soil stiffness and strength. In addition, the proportionality with $m_{\rm cone}$ indicates that when the cone is assumed to be narrower and strains are distributed over a larger depth, the characteristic length $c_q D$ increases.

The unknown gradient coefficient $m_{\rm cone}$ can be calculated to ensure compliance with other similarity models. For instance, in the case of a linear-elastic model where c_q is known [Eq. (4)], $m_{\rm cone}$ can be calculated by equating Eq. (4) with Eq. (12), for a smooth $(N_c = 5.69)$ and a rough $(N_c = 6.05)$ footing, respectively

$$m_{\text{cone}} = \frac{\pi}{4} (1 - \nu_s^2) N_c \approx 3.4 - 3.6$$
 (13)

This value of $m_{\rm cone}$ is used in the numerical applications given subsequently. Note that, this calibration of $m_{\rm cone}$ is higher than that given by Wolf and Deeks (2004), who derived a value of $m_{\rm cone} = \pi (1 - \nu_s) \approx 1.6$ for the vertical mode in incompressible soil. However, this value was calibrated for elastic settlement prediction and not in a similarity context.

Eq. (9) also enables nonlinear stress–strain functions to be employed to obtain analytical nonlinear pressure–settlement curves. For example, it can be assumed that the soil can be modeled using a hyperbolic soil constitutive model in the form

$$\frac{G_s}{G_i} = \left[1 + \frac{\gamma G_i}{s_u}\right]^{-1} \tag{14}$$

where $G_s(=\tau/\gamma)$ = secant shear modulus; and G_i = initial (low-strain) shear modulus. Substituting this function into Eq. (7) using the relationships below Eq. (9) and evaluating the integral yields the nonlinear pressure–settlement curve in flexibility form as follows:

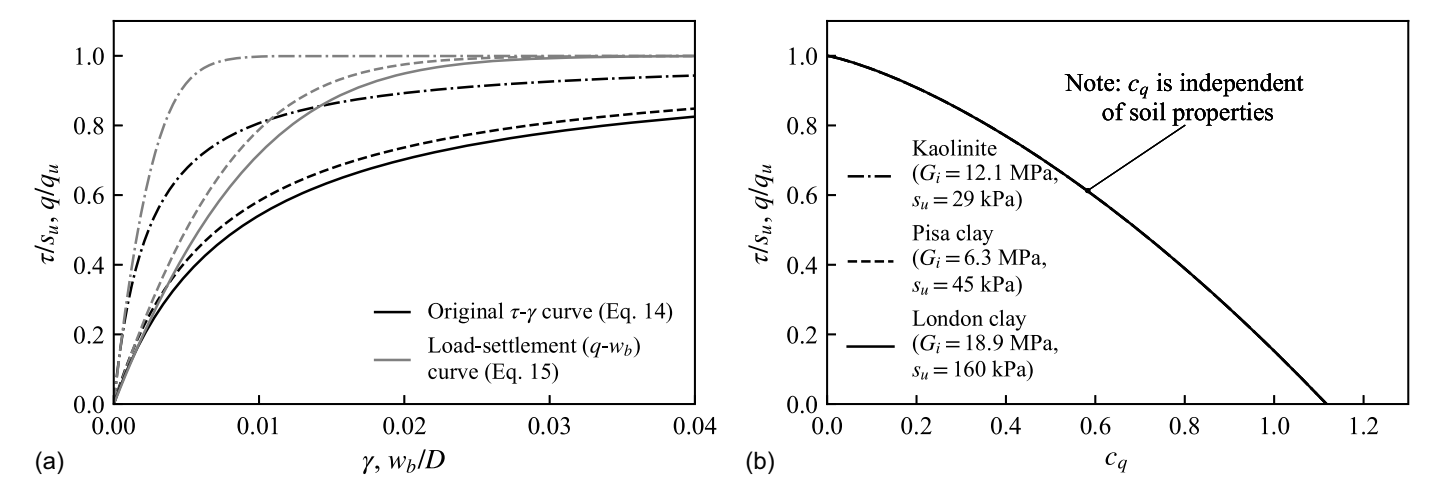


Fig. 4. Similarity results from the cone model approach using the hyperbolic soil constitutive model taking a smooth footing–soil interface ($\nu_s = 0.5$ and $N_c = 5.69$): (a) original normalized curves; and (b) the transformation factor. Soil parameters from Bateman (2025).

$$\frac{w_b}{D} = \frac{s_u \ m_{\text{cone}}}{2G_i(1 + \nu_s)} \sqrt{\frac{q}{q_u}} \left[\operatorname{arctanh} \left(\sqrt{\frac{q}{q_u}} \right) \right]$$
 (15)

Comparison of the constitutive model [Eq. (14)] and the pressure–settlement curve in Eq. (15) enables c_q to be obtained

$$c_q = \frac{m_{\text{cone}}(\frac{q_u}{q} - 1)}{2(1 + \nu_s)} \sqrt{\frac{q}{q_u}} \left[\operatorname{arctanh}\left(\sqrt{\frac{q}{q_u}}\right) \right]$$
 (16)

Remarkably, once again, c_q is independent of soil parameters G_i and s_u , but it depends on the geometry of the cone, the soil's Poisson's ratio and, most significantly, on the intensity of loading, q/q_u . This is plotted in Fig. 4 for three example soils, assuming $m_{\rm cone}$ from Eq. (13), as estimated previously. Example parameters for the hyperbolic soil model have been determined by Bateman (2025) by fitting this model to two triaxial tests from Soga (1994) in Pisa clay and kaolinite (Bateman et al. 2022b), as well as a third triaxial test in London clay by Gasparre (2005). The parameters for the three examples are shown in Fig. 4(b).

Additionally, a hyperbolic tangent (tanh) soil constitutive model is considered in the following form:

$$\gamma = \frac{\tau}{G_i} + \gamma_r \operatorname{arctanh}^2\left(\frac{\tau}{s_u}\right) \tag{17}$$

Substituting this equation into Eq. (7) [rearranged into vertical normal strains using the relationships below Eq. (9)] yields an integral whose solution could not be established in closed form. A numerical solution is presented in Fig. 5 for the same three example soils considered for the hyperbolic soil constitutive model. This results in the more complex c_q plot shown in Fig. 5(b), where, in addition to the aforementioned parameters q/q_u , ν_s , and $m_{\rm cone}$, the c_q value for this constitutive model also depends on G_i/s_u and γ_r . This result is unsurprising due to the addition of a parameter in the model.

The first point to observe is that for both the hyperbolic and tanh models, c_q varies with the applied load. At nearly zero load, both models start at a $c_q=1.12$, as per the elastic solution that $m_{\rm cone}$ was calibrated to, followed by a decrease of c_q with increased loading. This result aligns with the idea that a higher applied footing load results in increased strength mobilization and strain concentration in the area close to the footing, thus decreasing the characteristic dimension $(c_q D)$. The dependence of c_q on load intensity is a calibration parameter of the model and implies that perfect

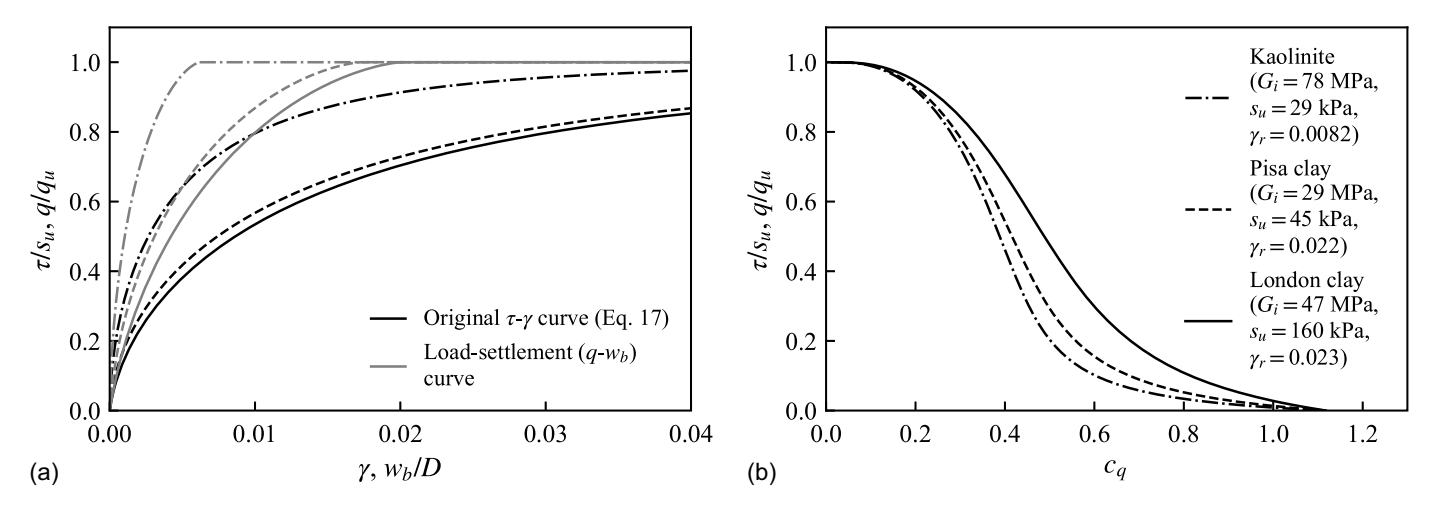


Fig. 5. Similarity results from the cone model approach using the tanh soil constitutive model taking a smooth footing–soil interface ($\nu_s = 0.5$ and $N_c = 5.69$): (a) original normalized curves; and (b) the transformation factor. Soil parameters from Bateman (2025).

similarity does not exist. However, an appropriate c_q may still be determined for a given range of q/q_u . The second observation involves the dependence of the transformation factor on the adopted soil model. In the case of a hyperbolic stress–strain relationship, there is no additional effect of soil parameters. However, in the case of the tanh model, a further variation of c_q is demonstrated for the different types of clay examined.

Discussion

A summary of the derived c_q values is shown in Fig. 6(a) for the classical similarity methods examined so far. Evidently, as shown by results from the novel cone model, c_q is likely dependent on the load intensity, the constitutive model and parameters, and the footing roughness.

Firstly, for approaching zero applied load, the elastic stiffness approach gives a single value of c_q [Eq. (4)] (1.12–1.19 for smooth and rough footings, respectively). In this work, these values are derived as closed-form expressions based on the original assumptions made by Skempton (1951). For higher stress regions, selection of an appropriate c_q value is more uncertain. Because geotechnical design practice usually involves safety factors equivalent to around two to three, the main stress region of interest is $q/q_u < 0.5$. Although significant variation of c_q values can be seen in this stress region in Fig. 6(a), the curves start from the aforementioned elastic value and decrease with increasing q/q_u values to an approximate range of $0.5 < c_q < 0.8$.

For a higher stress range $(q/q_u > 0.5)$, c_q can vary significantly and appears to approach zero. This implies that the normalized stress–strain curve for a given soil specimen asymptotes faster than the pressure–settlement curve that incorporates the response of soil over a wider area underneath the footing. At this stress range, similarity is unlikely to be applicable, and more complex analysis considering plasticity and failure should be sought.

Numerical Analysis

To explore the values of the linear transformation factor, c_q , idealized element tests can be compared to the pressure–settlement curves obtained from nonlinear numerical analysis. Osman et al.

(2007) considered vertical, horizontal, and moment loading on a pad foundation using this approach and updated the $M_c=1.35$ value obtained by Osman and Bolton (2005) to $M_c=1.25$, corresponding to $c_a=0.8$.

In this work, nonlinear numerical analysis was carried out in FLAC 2D (Itasca Consulting Group 2011) using (1) a hyperbolic soil constitutive model [Eq. (14)], and (2) a hyperbolic tangent (tanh) soil constitutive model [Eq. (17)]. These models were implemented in FLAC using the CPPUDM (user-defined) option using isotropic shear hardening. To this end, a Tresca yield surface was defined according to the mobilized soil shear strength. The evolution of the yield surface is controlled by a hyperbolic or tanh relationship, expressed in terms of plastic shear strain. This approach was undertaken for the three example soils discussed in the "Cone Model" section.

Numerical element–level undrained direct simple shear tests were initially conducted for the different soil types examined [model parameters and results shown in black in Figs. 7(a) and 8(a)]. These tests were undertaken to validate the accuracy of the model implementation at element level. Further validation of the boundary value problem examined herein was obtained by comparing the initial stiffness and ultimate values against available analytical solutions.

The footing pressure–settlement curves were obtained by applying a constant settlement rate to a rigid footing in large-scale axisymmetric-mode analyses [results shown in gray in Figs. 7(a) and 8(a)]. The model was set up with ~850 rectangular zones, with 10 grid points along the footing radius and the boundaries sufficiently extended to have negligible effect on the results. As expected, the pressure–settlement curve asymptotes toward an ultimate bearing capacity, q_u , which can be used to obtain the bearing capacity factor, N_c ($q_u = N_c s_u$ for undrained conditions). N_c of 5.58–5.61 (smooth) and 6.03–6.08 (rough) were obtained for both the hyperbolic and tanh models, all within 2% of the exact theoretical values from Shield (1955) and Eason and Shield (1960).

To obtain c_q , the y-axis of the stress-strain and the pressure-settlement curve are normalized by their ultimate capacities, taken from the numerical results (s_u and q_u , respectively). Comparing the two normalized curves enables c_q to be obtained as a function of load intensity. Figs. 7 and 8 show the numerical results for the hyperbolic and tanh models, respectively. Comparison with the

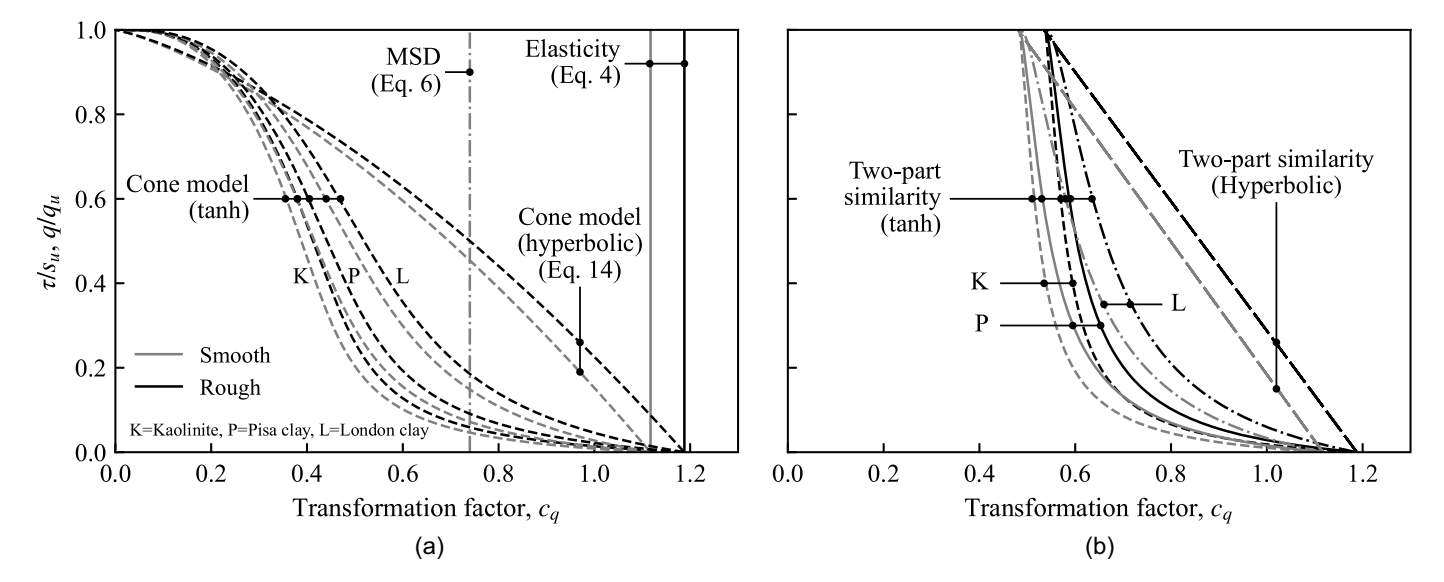


Fig. 6. Summary of c_q values obtained for (a) classical similarity; and (b) two-part similarity (smooth: $N_c = 5.69$; rough: $N_c = 6.05$).

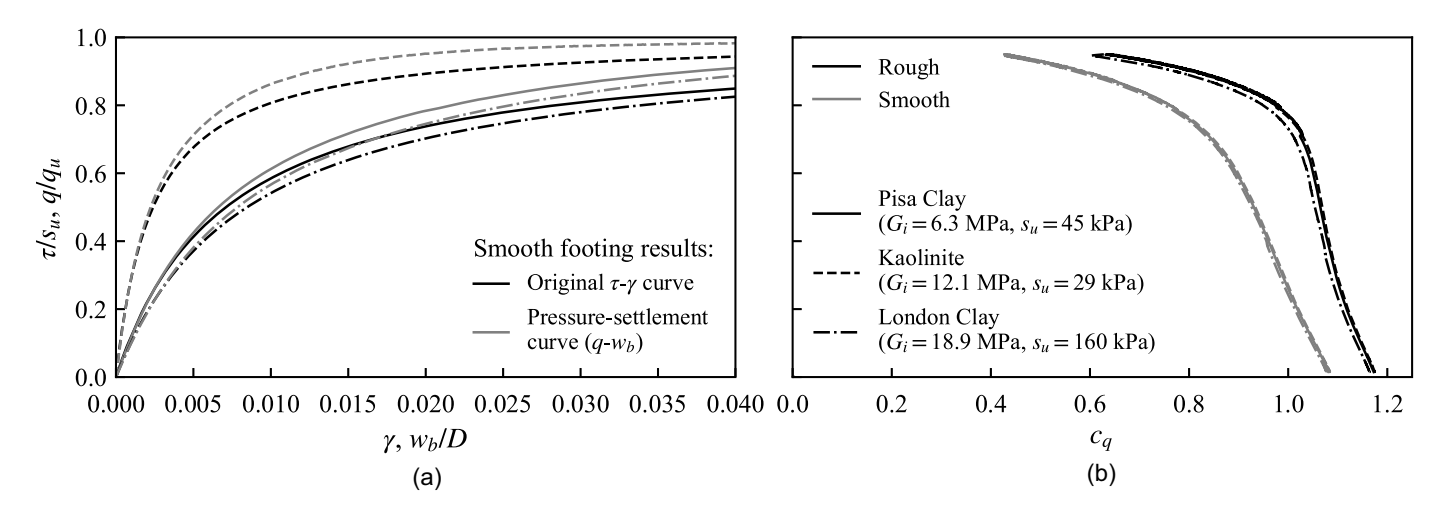


Fig. 7. Classical similarity results from FLAC 2D using the hyperbolic soil constitutive model: (a) stress–strain and pressure–settlement curves for a smooth footing (original normalized curves); and (b) resultant c_q values compared for smooth and rough footings. Soil parameters from Bateman (2025).

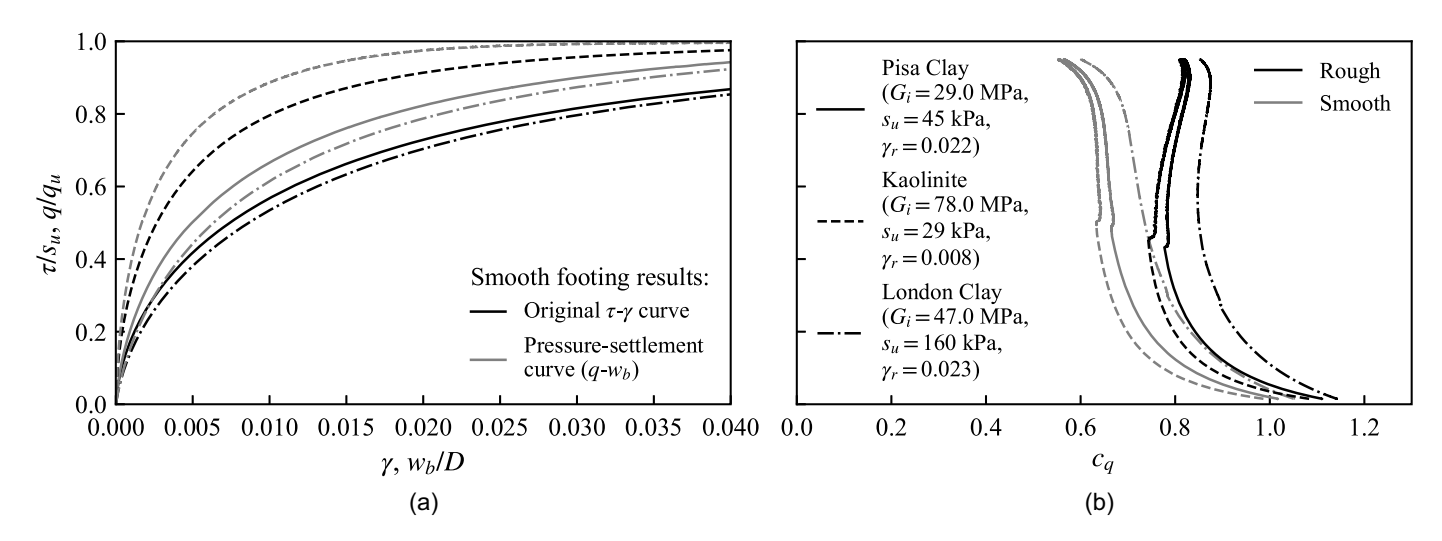


Fig. 8. Classical similarity results from FLAC 2D using the tanh soil constitutive model: (a) stress–strain and pressure–settlement curves for a smooth footing (original normalized curves); and (b) resultant c_q values compared for smooth and rough footings. Soil parameters from Bateman (2025).

corresponding results from the elastic and cone models (Fig. 4) indicate a very good match between the initial values of c_q and its variation with load intensity. The general trend of decreasing c_q with load intensity indicates that the size of the mechanism is decreasing, which aligns with the lower c_q value obtained from Osman and Bolton (2005) based on a smaller plastic displacement mechanism. Notably, the hyperbolic c_q results are essentially independent of soil properties.

Evidently, c_q is dependent on the roughness of the footing–soil interface. From the elasticity approach the c_q at low q/q_u values for a perfectly rough footing are approximately 5% larger than that of a smooth footing. The numerical results indicate that c_q for a rough footing decreases slower with load intensity than that for a smooth footing.

Elastic-Perfectly Plastic Model Paradox

Both soil constitutive models employed in the FLAC analyses asymptoted toward an undrained shear strength s_u . However, numerical models with an elastic-perfectly plastic response are often used in geotechnical practice (e.g., the Mohr-Coulomb soil model).

If such a model is selected, the c_q factor at zero loading starts from an elastic value that remains consistent with the results discussed in the preceding sections. This is shown in Fig. 9, which summarizes the results of FLAC analyses with the Mohr-Coulomb model. The elastic c_q value was maintained until a loading intensity of approximately $0.3q/q_u$, at which point yielding of soil elements under the footing started occurring. From this point onward, the pressuresettlement curve asymptoted toward the ultimate bearing capacity of the footing, but the stress–strain curve remained linear-elastic until the undrained shear strength was reached. The transformation factor c_q increased toward a maximum value of

$$c_{q,u} = \frac{w_{b,u}}{\gamma_u D} \tag{18}$$

where $w_{b,u}$ = settlement at failure of the footing; γ_u = failure strain of the soil and $c_{q,u}$ = c_q value at q/q_u = 1. As a result, when γ_u is finite (as per the Mohr-Coulomb model) and the pressure–settlement curve asymptotes toward infinite settlement, c_q approaches infinity at large applied loads.

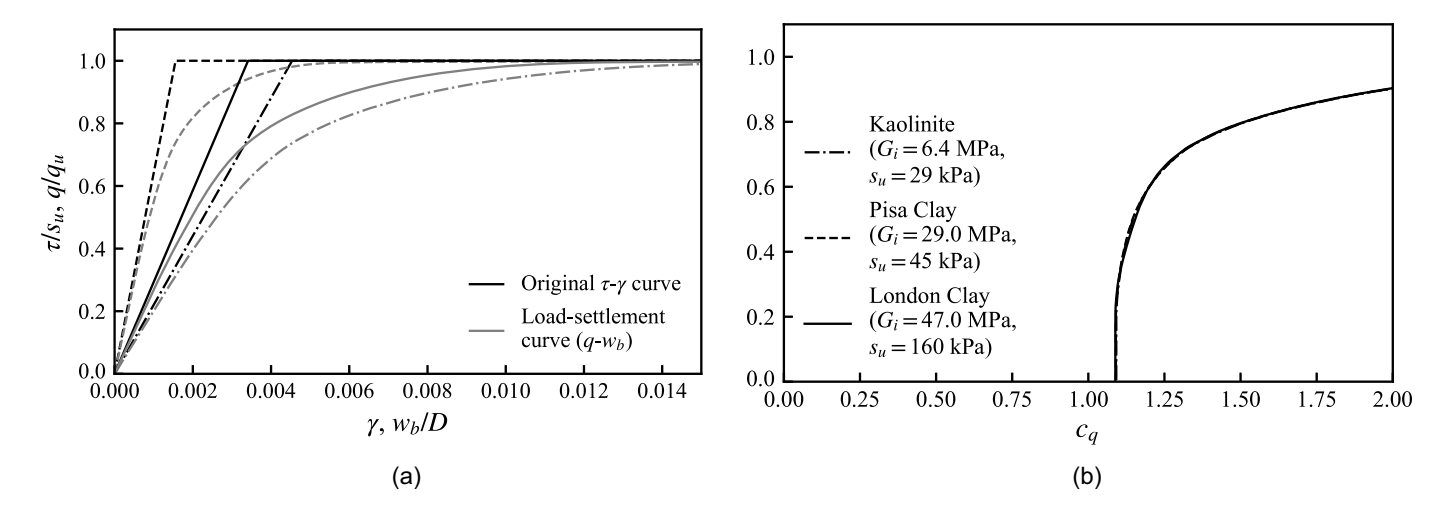


Fig. 9. Classical similarity results from FLAC 2D using the Mohr-Coulomb soil constitutive model assuming a smooth footing–soil interface: (a) stress–strain and pressure–settlement curves (original normalized curves); and (b) resultant c_q values. Soil parameters from Bateman (2025).

Evidently, any elastic-perfectly plastic model would significantly underpredict the failure strain, or alternatively, overpredict the initial stiffness G_i . Therefore, this increase of the transformation factor c_q is unrealistic, and such models should be avoided in the context of similarity.

Sensitivity to N_c

To employ the similarity approach, the applied pressure is factored by N_c to get the shear stress to input into the representative soil sample. Although the N_c values provided by Shield (1955) are exact, the solutions for noncircular or slightly embedded foundations are not. This, in addition to soil heterogeneity and the nonlinearity of the foundation response, means these exact values may not match field test results. In light of this uncertainty, the effect of selecting an inaccurate N_c has been investigated with an example analysis in FLAC using both a hyperbolic and a tanh soil constitutive model. As shown in Fig. 10(a), the same pressure–settlement curve from the surface footing in FLAC is normalized against N_c values that have been underpredicted or overpredicted by 10%.

Fig. 10(b) demonstrates that the error in the c_q propagates to the prediction of the elastic low-load value of the transformation factor, with the underestimation of N_c resulting in underpredictions of c_q (and consequently foundation settlement) by an equal percentage, and vice versa.

Two-Part Similarity

As discussed in the preceding sections, it is evident from the results that perfect similarity across the full loading range is unlikely, and instead, c_q appears to decrease with increased load intensity. To tackle this issue, one possible solution is to adopt a two-part similarity procedure that employs separate scaling factors for the elastic and plastic components of strain in the normalized stress–strain curve, to produce the corresponding elastic and plastic components of displacement in the normalized pressure–settlement curve. Comparable to Eq. (1), this can be written

$$\frac{w_b}{D} = \frac{w_{b,e}}{D} + \frac{w_{b,p}}{D} = c_{q,e} \gamma_e + c_{q,p} \gamma_p \tag{19}$$

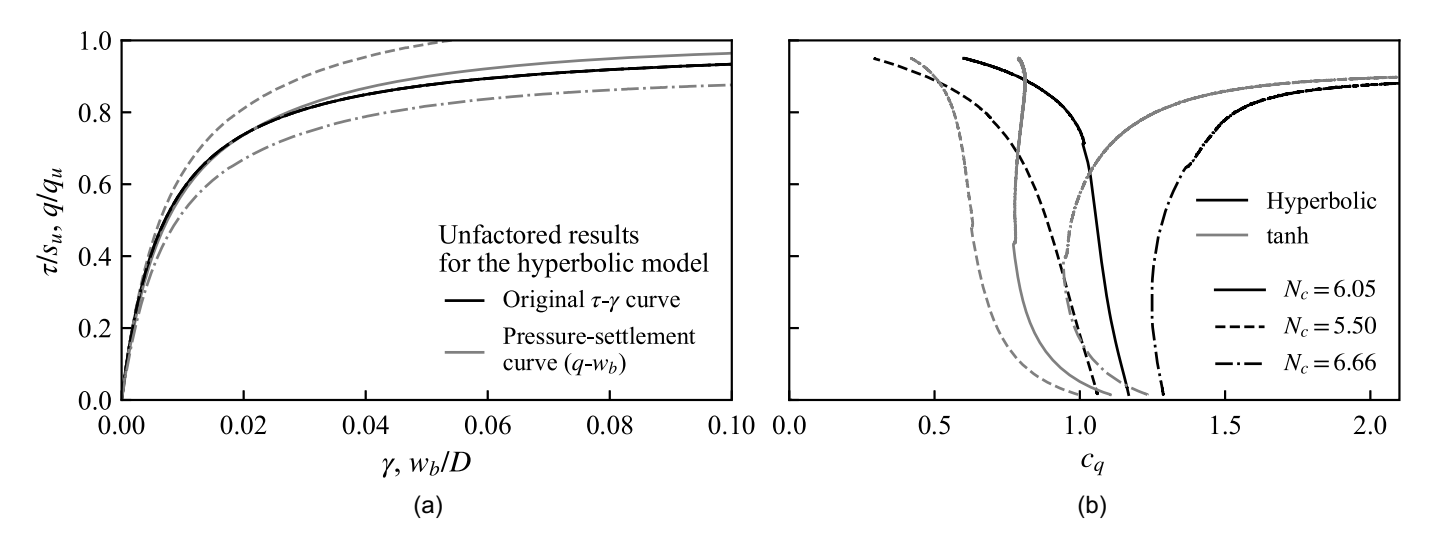


Fig. 10. Effect of selecting an incorrect N_c on c_q using the hyperbolic constitutive model ($G_i = 6.3$ MPa and $s_u = 45$ kPa) in FLAC 2D: (a) original normalized curves; and (b) transformation factor.

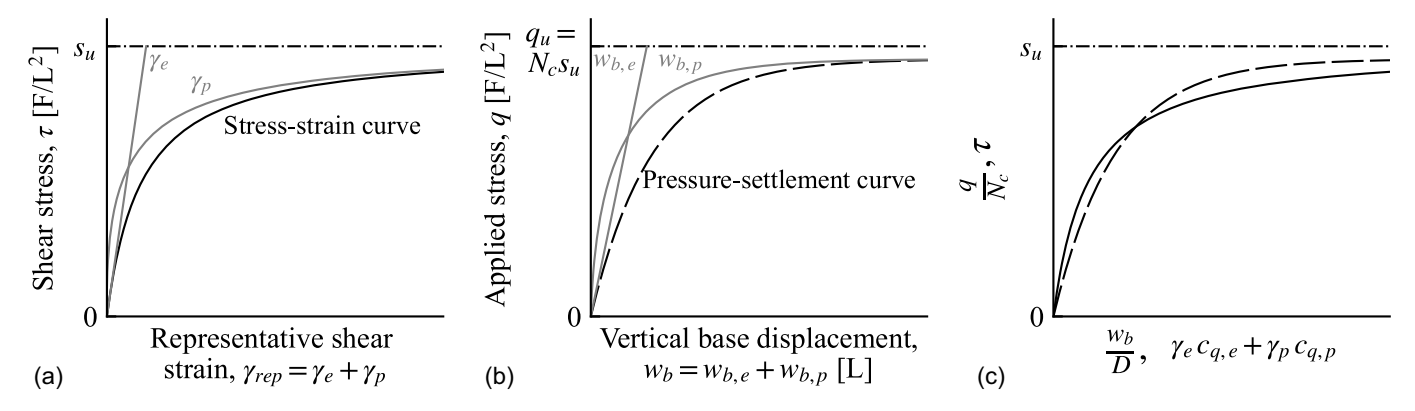


Fig. 11. Illustration of the two-part similarity approach: (a) idealized stress-strain curve from an element test of a representative soil sample split into elastic and plastic components; (b) idealized pressure-settlement curve split into elastic and plastic components; and (c) normalized and transformed curves seeking similarity.

where γ_e and γ_p = elastic and plastic components of the soil shear strains; $w_{b,e}$ and $w_{b,p}$ = elastic and plastic components of settlement; and $c_{q,e}$ and $c_{q,p}$ = corresponding elastic and plastic linear transformation factors, respectively. This approach is shown in Fig. 11.

In a similar way to the classical similarity approach, to employ this method in design (after appropriate $c_{q,e}$ and $c_{q,p}$ values are selected), the following simple steps should be used:

- 1. Divide q, the pressure applied to the foundation, by N_c to get $\tau_{\rm ref}$, the equivalent shear stress on the representative soil sample.
- Split the representative soil element test into the elastic and plastic components using G_i.
- 3. Use this soil element test to obtain the elastic strain γ_e and the plastic strain γ_p in the representative soil sample at $\tau_{\rm ref}$, the equivalent shear stress.
- 4. Use Eq. (19) to obtain the foundation displacement w_b under the applied pressure q.

Step 2 requires the value of G_i to be known, a soil parameter often hard to determine in the laboratory without special equipment (e.g., a resonant column or bender element tests). However, this is typically easier to obtain with in situ methods, such as correlating with cone penetration test (CPT) results or through geophysical testing [such as spectral analysis of surface waves (SASW); and multichannel analysis of surface waves (MASW)] [Foti et al. (2015) has given more details].

Equivalent values for $c_{q,e}$ and $c_{q,p}$ have previously been derived for curves relating to axially and laterally loaded piles (e.g., Fu et al. 2020; Jeanjean et al. 2017). This approach has also been used implicitly by Jakub (1977), who assumed that a secant stiffness—stress curve can be given in the same form as a secant stiffness—load curve for a strip footing under dynamic horizontal/moment loading. Because the two-part similarity approach has not been explicitly applied to a vertically loaded footing in axisymmetric mode, this paper will go on to extend the method employed by Jakub (1977) to obtain novel $c_{q,e}$ and $c_{q,p}$ values for the particular case.

Jakub-Roesset Method

Working with Roesset, Jakub (1977) suggested that lateral load—displacement curves and moment—rotation curves for strip footings can be given in the same functional form as a stress—strain curve. Jakub (1977) employed a Ramberg-Osgood soil constitutive model, given by

$$\frac{G_s}{G_i} = \frac{\tau}{\gamma G_i} = \frac{1}{1 + a \left(\frac{\tau}{s_u}\right)^{b-1}} \tag{20a}$$

$$\gamma = \gamma_e + \gamma_p = \frac{\tau}{s_u} \frac{s_u}{G_i} + a \frac{s_u}{G_i} \left(\frac{\tau}{s_u}\right)^b \tag{20b}$$

where G_s and G_i = secant and initial (or low-strain) shear modulus, respectively; $a = \gamma_{pf}G_i/s_u$ is a fitted model parameter corresponding to the plastic shear strain at failure, γ_{pf} ; and b = model exponent. This model does not asymptote to an ultimate value but requires a cap at s_u (see "Elastic-Perfectly Plastic Model Paradox" section).

Following the assumption of Jakub (1977), the corresponding pressure–settlement curve is given by

$$\frac{K_s}{K_i} = \frac{q}{w_b K_i} = \frac{1}{1 + \chi a(\frac{q}{a})^{b-1}}$$
 (21a)

$$w_b = \frac{q}{q_u} \frac{N_c s_u}{K_i} + \chi a \frac{N_c s_u}{K_i} \left(\frac{q}{q_u}\right)^b \tag{21b}$$

where K_s and K_i = secant and initial stiffness of the pressure–settlement curve, respectively ($K_s = q/w_b$); and χ = fitting parameter discussed below.

Evidently, both Eqs. (20b) and (21b) are naturally split into the elastic and plastic portion of the curves. Furthermore, the assumption that Eqs. (20a) and (21a) can be given in the same form is equivalent to assuming a two-part similarity. Therefore, $c_{q,e}$ and $c_{q,p}$ can be calculated directly [substituting in $K_i = 8G_i/(\pi(1-\nu_s)D)$ from Eq. (3)] as follows:

$$c_{q,e} = \frac{w_{b,e}}{\gamma_e D} = \frac{\pi}{8} (1 - \nu_s) N_c$$
 (22a)

$$c_{q,p} = \frac{w_{b,p}}{\gamma_p D} = \chi \left[\frac{\pi}{8} (1 - \nu_s) N_c \right] = \chi c_{q,e}$$
 (22b)

As expected, $c_{q,e}$ [Eq. (22a)] is identical with the elasticity solution for c_q in Eq. (4).

Jakub (1977) originally suggested determining χ by fitting Eq. (21) to numerical pressure–settlement curves obtained using a Ramberg-Osgood model simplified by setting b=2. This is undertaken here using FLAC 2D following the same method as discussed in the "Numerical Analysis" section. Following the assumption that the pressure–settlement curve can be given in the form of Eq. (21), plotting $K_i w_b/q$ against aq/q_u would be expected to result in a straight line with a gradient χ and an intercept at q=0 defined by $K_i=K_s$ [Fig. 12(a)]. Evidently, this assumption is not perfect, but a simple linear regression can be applied to obtain χ . The results are plotted in Fig. 12(a) for

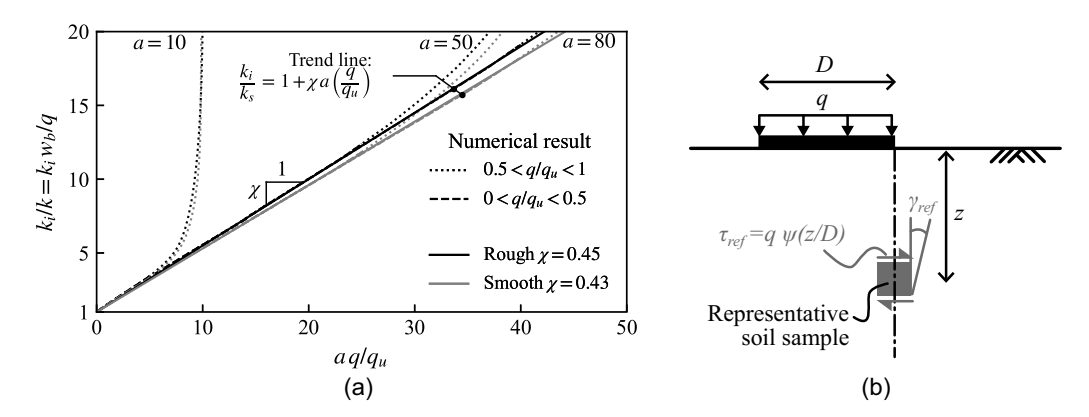


Fig. 12. (a) Interpretation of χ (b=2); and (b) representative soil sample definition.

different a values, with interpreted trend lines shown. These give $\chi=0.45$ and $\chi=0.43$ for rough and smooth footings, respectively, which correspond to $c_{q,p}=0.53$ and $c_{q,p}=0.48$ [Eq. (22b)]. For preliminary analysis, Jakub (1977) suggested that these values can be also used in cases with alternative b values or even for different constitutive models.

Given $c_{q,e}$ and $c_{q,p}$ in the form of Eqs. (22a) and (22b), an equivalent value of the classical c_q can be obtained

$$c_q = \frac{w_b}{\gamma D} = \frac{c_{q,e} \gamma_e + c_{q,p} \gamma_p}{\gamma_e + \gamma_p} \tag{23}$$

Eq. (22) suggests that $c_{q,e}$ and $c_{q,p}$ are constant with applied load. The low-stress region is governed by $c_{q,e}$ because $\gamma_p=0$ as the applied load approaches zero. However, the variation of c_q with increased applied loads is governed by the value of $c_{q,p}$. Evidently, if $c_{q,p} < 1$ [suggested by the fit in Fig. 12(a)], this would suggest that c_q decreases with increased applied load. Remarkably, this agrees with the results presented for the classical similarity method and has the additional benefit of being controlled by a constant $c_{q,p}$.

Applying Eq. (23) to the hyperbolic and tanh models [Eq. (14) and (17), respectively] results in c_q values that can be compared with those obtained previously. Assuming that χ can be given by those obtained in Fig. 12(a), the resulting values are plotted in Fig. 6(b).

Representative Soil Sample

Jakub (1977) also proposed rewriting the footing secant stiffness [Eq. (21a)] in an alternate form

$$\frac{K_s}{K_i} = \frac{q}{w_b K_i} = \frac{1}{1 + a(\frac{\tau_{\text{ref}}}{S_{s,i}})^{b-1}}$$
 (24)

where $\tau_{\rm ref}$ = shear stress at a reference location at a certain depth below the edge of the footing. This is illustrated in Fig. 12(b) and allows converting χ into a reference location (for b=2), resulting in

$$\chi = N_c \frac{\tau_{\text{ref}}}{q} = N_c \psi \left(\frac{z}{D}\right) \tag{25}$$

where $\psi(z/D)=\tau_{\rm ref}/q$ describes the dimensionless attenuation of shear stress with depth.

For lateral loading in plane-strain conditions, Jakub (1977) proposed that the representative soil element is located at z=0.25D under the edge of the footing. This is notably similar to a depth of

z=0.3D for the vertical mode suggested independently by Osman and Bolton (2005) in the context of the MSD method. Assuming a depth of z=0.3D in the problem examined here, the corresponding dimensionless attenuation can be obtained from Poulos and Davis (1974) as $\psi(z/D)=0.23$, leading to $c_{q,p}=1.6$. This is substantially higher than the values of 0.48 to 0.53 presented previously. On the other hand, the values of χ obtained in Fig. 12(a) correspond to attenuation coefficients approximately $\psi=0.08$, which would apply to locations of the representative soil sample between z=0.9D and 1D below the edge of the footing. This is much deeper than the representative soil element location suggested by Osman and Bolton (2005) from the MSD approach.

Numerical Analysis

As a comparison to the $c_{q,p}$ values determined using the Jakub-Rosett method previously, $c_{q,p}$ can also be interpreted directly from the numerical results obtained previously. As expected, the elastic component $c_{q,e}$ is consistent with the value of c_q at zero loading. To obtain $c_{q,p}$, the y-axis of the stress–strain and pressure–settlement curves are normalized by their ultimate capacities, taken from the numerical results (s_u and q_u , respectively), similar to what was done when using classical similarity. However, the predicted elastic component of the corresponding strain/displacement is also subtracted from the original x-axis value for the hyperbolic and tanh models calibrated to the three example soils, respectively. Comparing the two normalized curves (with elastic portions removed) enables $c_{q,p}$ to be obtained as a function of load intensity. This was done for rough and smooth footings, shown in Fig. 13.

The numerical results shown in Fig. 13 were compared with the values obtained using the Jakub-Roesset method. The numerical results in Fig. 13 showed less variation of $c_{q,p}$ with load intensity than observed for c_q in the classical similarity method [Figs. 7(b) and 8(b)]. This good agreement applies over a wider range of load intensity when compared with the classical similarity solutions, possibly as high as $q/q_u=0.8$.

Stiffness Similarity

An alternative similarity method has been proposed by Atkinson (2000), who suggested that similarity in shape exists between (1) the secant shear modulus degradation of a soil element with increasing strain $(G_s-\gamma)$, and (2) the secant stiffness decay of a surface foundation with increasing normalized settlement $(K_s - w_b/D)$. This will be denoted herein as *stiffness similarity*

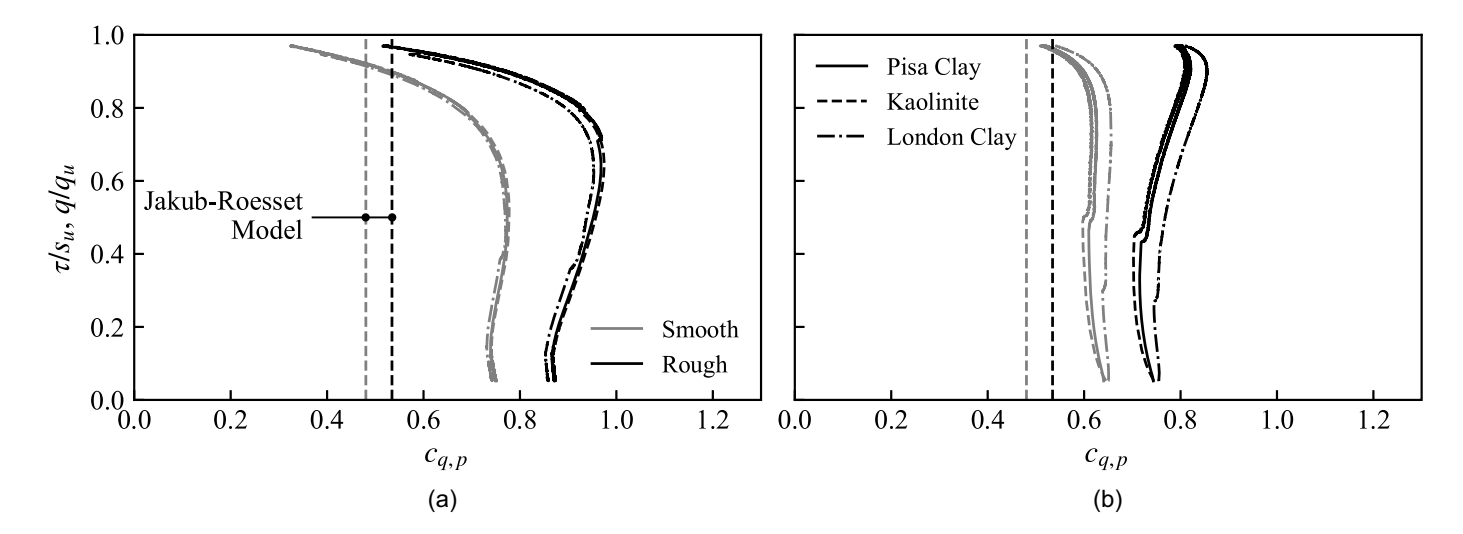


Fig. 13. Values $c_{q,p}$ obtained from FLAC 2D for (a) hyperbolic; and (b) tanh soil constitutive models. Soil parameters given in Figs. 7 and 8.

and is employed in a similar manner to the classical similarity method suggested by Skempton (1951).

Firstly, the two curves are normalized by their ultimate values, naturally bounding the curves between zero and one on the y-axis. These are the initial (low-strain) shear modulus, G_i , and the initial stiffness of the pressure–settlement curve, K_i , respectively. This is given by the Boussinesq solution in Eq. (3) when $G = G_i$. Therefore, the linear transformation factor of the y-axis is given by

$$\frac{K_i}{G_i} = \frac{8}{\pi (1 - \nu_s)} \tag{26}$$

Secondly, the abscissa (x-axis) of the G_s - γ curve is factored (stretched or compressed) by a characteristic dimension, typically selected to be proportional to the footing diameter, D. This method is illustrated in Fig. 14. The linear transformation of the x-axis can be expressed by

$$\gamma_{\text{rep}} = \frac{w_b}{c_{q,s}D} \tag{27}$$

This linear transformation factor, $c_{q,s}$, appears to be in the same form as Eq. (1), namely defining a characteristic dimension, $c_{q,s}D$, normalizing the footing settlement, w_b . However, the derived transformation factors using the two similarity approaches (c_q from the "Classical Similarity" section and $c_{q,s}$ here) cannot be directly

compared because the form of the soil element test that is scaled is not the same.

Unlike the previous similarity approaches discussed, the stiffness similarity approach does not allow an engineer to start with an applied foundation pressure and estimate the settlement. Instead, after an appropriate $c_{q,s}$, is determined, the following simple steps should be employed [Atkinson (2000) has given more details]:

- 1. Choose an allowable settlement w_b/D (normalized by the footing diameter).
- 2. Divide the normalized settlement by $c_{q,s}$ to calculate the representative shear strain within the soil [Eq. (27)].
- 3. Use a representative soil element test (or assumed constitutive model) to obtain the secant shear modulus in the representative soil sample, G_s , at this representative shear strain.
- 4. Use the Boussinesq equation [Eq. (3)] to calculate the allowable pressure that can be applied to the foundation.

If the settlement at a known applied pressure is desired instead, these steps can be applied iteratively. Step 4 is equivalent to applying the scaling factor in Eq. (26) to the secant shear modulus, G_s , to calculate the secant stiffness of the footing, K_s , and then multiplying by the normalized footing settlement, w_b/D .

Atkinson (2000) compared empirical settlement values for surface (and piled raft) footings on London clay with triaxial tests undertaken in the same material (for $0.05 < K_s/K_i < 0.25$). Atkinson (2000) did this by calculating equivalent undrained secant Young's modulus values for the footing using the bearing pressure

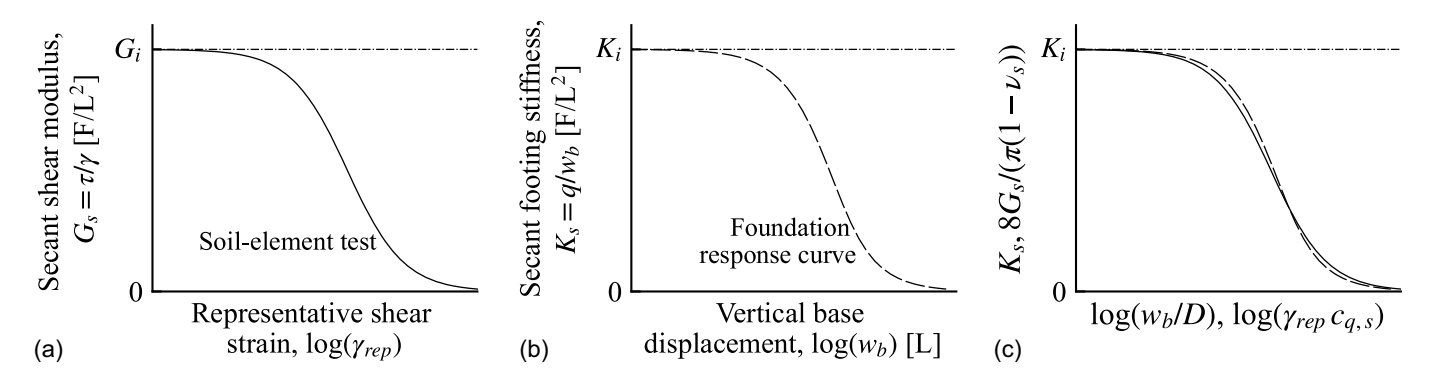


Fig. 14. Stiffness similarity concept: (a) idealized modulus reduction curve from an element test of a representative soil sample; (b) idealized stiffness reduction curve of a foundation; and (c) normalized and transformed curves seeking similarity.

and observed settlement in Eq. (3). This is equivalent to the method discussed previously. From this comparison, Atkinson (2000) established that the normalized foundation settlement was three times larger than the corresponding axial strains from the triaxial test. This is equivalent to $c_{q,s} \approx 2$ for an undrained material because the linear transformation factor in this work is applied to shear strain rather than axial strain. This value was then verified by Atkinson (2000) using centrifuge modeling on kaolin clay (for $0.05 < K_s/K_i < 0.6$) and model plate load tests in sand (for $0.05 < K_s/K_i < 0.75$). Further validation was subsequently provided by Osman et al. (2007) using nonlinear FEA.

In the classical similarity approach the y-axis is normalized by the capacity, which means an elasticity solution is used to derive a c_q value. However, in the stiffness similarity approach, the y-axis is normalized by an elasticity solution, which means it cannot be employed to analytically derive $c_{q,s}$, and the predicted capacity can be used instead. In both the classical and stiffness similarity solutions, these analytical methods are both equivalent to matching the intersection between the elasticity solution and the capacity, i.e., the yield point in an elastic-perfectly plastic model. In the stiffness similarity case, the normalized stiffnesses for the soil element and the footing after yield are

$$\frac{G_s}{G_i} = \frac{s_u}{G_i} \left(\frac{1}{\gamma}\right) \tag{28a}$$

$$\frac{K_s}{K_i} = \frac{q_u}{K_i} \left(\frac{1}{w_b} \right) \tag{28b}$$

where K_i can be found using the Boussinesq solution [Eq. (3)]. Therefore

$$c_{q,s} = \frac{w_b}{\gamma D} = \frac{\pi}{8} (1 - \nu_s) N_c \tag{29}$$

More specifically, this would yield a $c_{q,s}$ of 1.12 and 1.19 for smooth and rough footings, respectively. Despite being identical to the c_q calculated in Eq. (4), there cannot be a direct comparison between these cases. Firstly, this is because classical similarity is performed on the basis of stress–strain and pressure–settlement curves, whereas stiffness similarity is applied on secant shear modulus and foundation stiffness degradation. Secondly, the transformation factor in Eq. (4) refers to small load intensities $q/q_u \rightarrow 0$, whereas Eq. (29) corresponds to loading close to failure $q/q_u \rightarrow 1$.

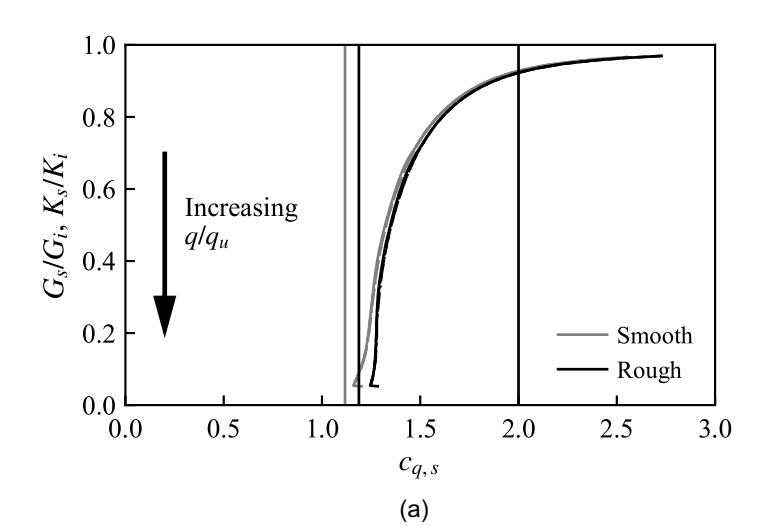
In addition to the analytical validation presented herein, this paper proceeds to evaluate the applicability of the stiffness similarity method by calculating $c_{q,s}$ values from the FLAC analysis conducted (both for hyperbolic and tanh model). The results are shown in Fig. 15. As can be observed, the $c_{q,s}$ value rapidly approached infinity at low strain ranges (where G_s is still close to G_i , i.e., $G_s/G_i > 0.9$), where the classical similarity approach may be more applicable. For $0.2 < G_s/G_i < 0.8$, $c_{q,s}$ can be seen to be in the range $0.8 < c_{q,s} < 1.5$ for the hyperbolic model and obtained a slightly higher range of approximately $1.2 < c_{q,s} < 2$ for the tanh model. Interestingly, in general, the two models were bounded by the elastic perfectly plastic solution and the proposed value from Atkinson (2000).

Case Study

Three case study examples are provided to illustrate the use and applicability of the three similarity methods investigated in this paper: (1) classical similarity, (2) two-part similarity, and (3) stiffness similarity. The various similarity factors determined in the aforementioned sections have been employed and compared. The three examples considered include both pressure–settlement curves from vertically loaded footings as well as triaxial test data from the same site. Details about each case are discussed in the following subsections.

Bothkennar

Firstly, Jardine et al. (1995) obtained vertical pressure–settlement curves from rigid pad foundations in Bothkennar (Scotland) on clays and silts. Full details about the material are provided in the original paper and other publications from the site (Hight et al. 1992a, b; Allman and Atkinson 1992; Nash et al. 1992). Jardine et al. (1995) conducted tests on two reinforced concrete foundations cast at a depth of 0.8 m. Pad A was loaded to failure under short-term loading conditions and thus was selected for use in this case study. The footing is 2.2 m square, with an estimated equivalent diameter of 2.48 m (Jardine et al. 1995) and is assumed perfectly rough. Following the original paper, a N_c value of 6.1 (Eason and Shield 1960) can be corrected for a depth of 0.8 m using the Brinch Hansen (1970) depth correction factor [1 + 0.4z/D], giving an overall $N_c = 6.9$. The pressure–settlement curve is shown in



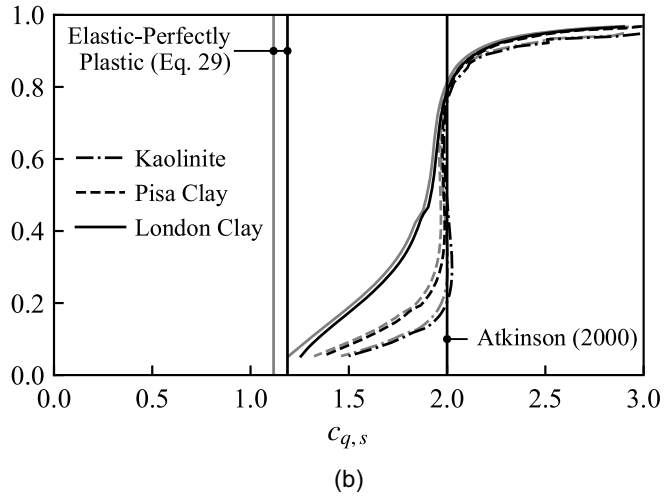


Fig. 15. Values of $c_{q,s}$ obtained from FLAC 2D for (a) hyperbolic; and (b) tanh soil constitutive models. Soil parameters are given in Figs. 7 and 8.

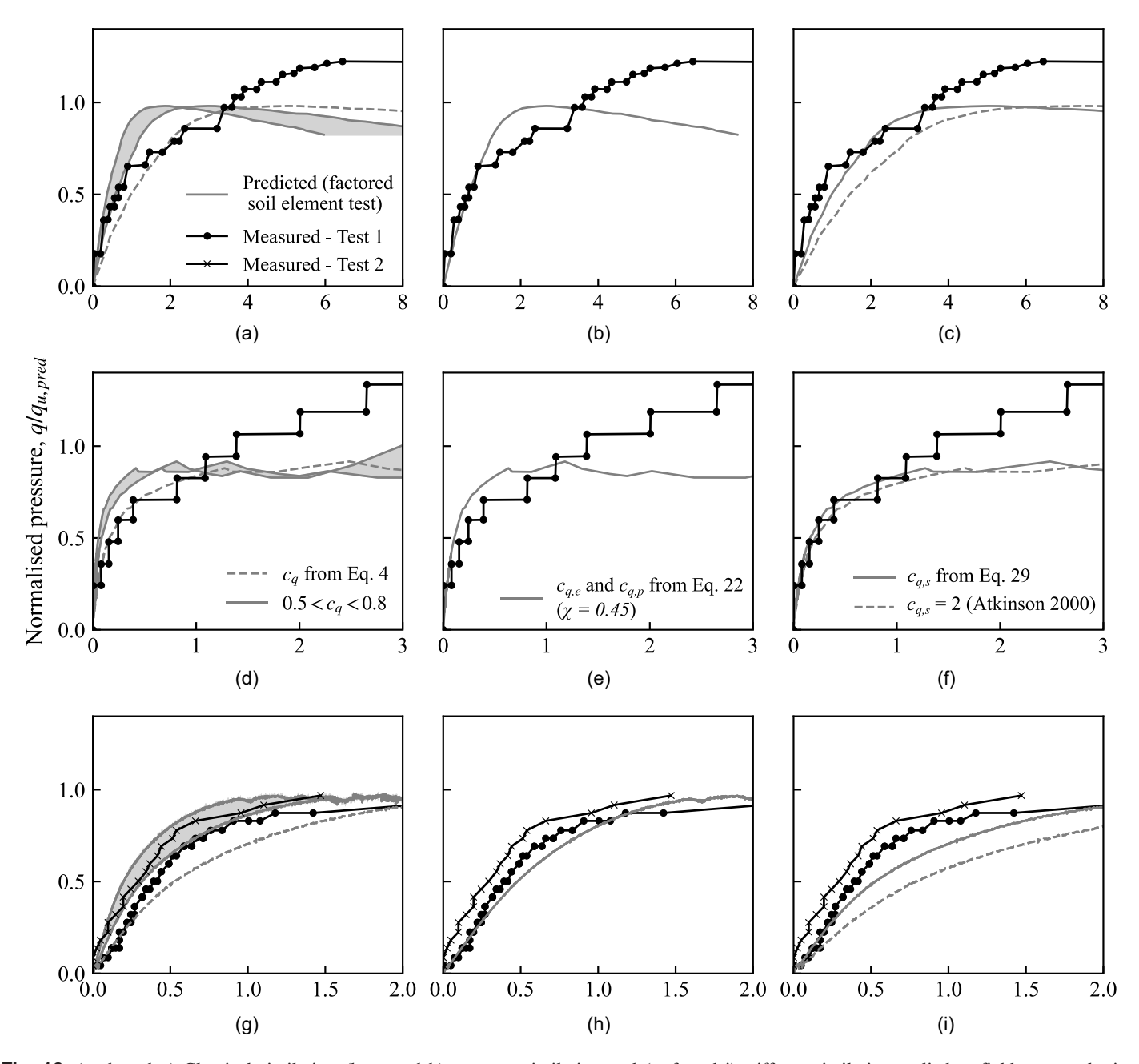


Fig. 16. (a, d, and g) Classical similarity; (b, e, and h) two-part similarity; and (c, f, and i) stiffness similarity applied to field test results in (a–c) Bothkennar clay; (d–f) Kinnegar silt; and (g–i) soft clay near Ballina. Note, the equivalent diameter D = 1.13B is used where the test footing is square, where B is the footing width. (Data from Jardine et al. 1995; Hight et al. 1992a; Lehane 2003; Doherty et al. 2018a, b.)

Figs. 16(a–c) (in black), which approaches an ultimate stress, q_u , of 138 kPa.

Undrained triaxial compression and extension tests were undertaken by Hight et al. (1992a) in Bothkennar clay at multiple depths. Because the s_u value increases with depth, it is important to select a representative soil sample. Given $N_c=6.9$, a representative undrained shear strength of $s_u\approx 20$ kPa should be employed. This occurs at a depth of approximately 1.6 to 2.7 m (0.3 < z/D < 0.8). Therefore, an undrained triaxial compression test using a Sherbrooke sampler at a depth of 2.67 m was selected as the only test within this depth region. However, $s_u=16$ kPa was obtained from this test, resulting in a predicted capacity of $q_u=108$ kPa (used to normalize the results). Where relevant, an initial shear modulus, G_i , value of 3 MPa was used, as obtained from

pressuremeter tests detailed by Hight et al. (1992b), and K_i was determined theoretically from Eq. (3).

The predicted N_c value (6.9) was multiplied by the s_u obtained from the soil element test to predict the capacity of the footing. This value was used to normalize both the field test and the predicted pressure–settlement curve $(q_{u,pred} = N_c s_u)$.

Kinnegar

Secondly, a vertically loaded footing test was undertaken by Lehane (2003) at Kinnegar in Northern Ireland. The footing was cast at 1.6-m depth on a silty stratum. Full details of the material properties have been provided by Lehane (2003). The footing consisted of a 2-m-square 1.7-m-thick reinforced concrete footing,

which was assumed here to have an equivalent circular diameter of 2.26 m (Osman and Bolton 2005). Following the original paper, a N_c value of 6.2 (using a shape correction factor of 1.2 and an inclination factor of 0.98) can be corrected for a depth of 1.6 m using the Brinch Hansen (1970) depth correction factor [1+0.4z/D], giving an overall $N_c=7.8$. The pressure–settlement curve is shown in Figs. 16(d–f), which approaches an ultimate stress, $q_u=96.5$ kPa.

Lehane (2003) also presented an undrained triaxial compression test on the silt, presented in secant stiffness form, normalized by the initial mean effective stress (30 kPa as per the original paper). A triaxial test from the recommended depth beneath the footing is not available. This interpretation results in s_u of 9.2 kPa, resulting in a predicted capacity of $q_{u,\text{pred}}=60$ kPa (used to normalize both the field test results and predicted pressure–settlement curve). Where relevant, an initial shear modulus, $G_i=11.8$ MPa was selected as the maximum measured shear modulus in the triaxial test, and the corresponding K_i was determined theoretically from Eq. (3).

Ballina

Finally, two vertically loaded footing tests were undertaken by Gaone et al. (2018) at the Australian National Field Testing Facility (NFTF), near Ballina, Australia. Full details of the site investigation are provided by Doherty et al. (2018b). The footings consisted of a 1.8-m square (assumed equivalent to a 2.04-m-diameter circular footing) constructed at a depth of 1.5 m in a pit on soft clay. Doherty et al. (2018a) interpreted a $q_u = 63$ kPa. The pressuresettlement curves are shown in Figs. 16(g-i).

Undrained triaxial compression tests from the site are available from Doherty et al. (2018a, b). A triaxial test taken at a depth below the footing of 0.3D [as suggested by Osman and Bolton (2005)] was selected, which resulted in $s_u = 10.5$ kPa. Taking $N_c = 5.69$ and applying a shape factor of 1.2 gave $N_c = 6.8$ and yielded $q_u = 67$ kPa, used to normalize the results. Where relevant, $G_i = 1,600$ kPa was assumed (Doherty et al. 2018a), and the corresponding K_i was determined from Eq. (3).

Application of Similarity

For each example, the three similarity approaches were employed. For classical similarity, the pressure–settlement and stress–strain curves were normalized by N_c (discussed previously). The shear strain of the triaxial test was then scaled by different c_q values, discussed previously. Firstly, the strain was scaled by c_q from Eq. (4) suggested for very low stress $(q/q_u < 0.05)$, and secondly, by a range of $0.5 < c_q < 0.8$, as suggested for medium stress levels $(q/q_u \approx 0.5)$. The resulting transformed normalized stress–strain curves are compared with the corresponding normalized pressure–settlement curves in Figs. 16(a, d, and g) for the three case study examples.

Two-part similarity is employed by separating the elastic and plastic components of the stress–strain curve. The elastic portion (calculated using G_i) and plastic portions (remaining after subtracting the elastic component) are scaled by Eqs. (22a) and (22b) (setting $\chi=0.45$), respectively. The results are shown in Figs. 16(b, e, and h) for the three case studies.

Finally, stiffness similarity is performed by converting the triaxial test stress–strain curve into the stiffness space ($G_{\text{sec}} = \tau/\gamma$) and scaling the shear strain of the triaxial test by the different $c_{q,s}$ values to get w_b/D . The curves are scaled by $c_{q,s}$ from Eq. (29) (suggested in this work for very high stress, $q/q_u=1$), and by $c_{q,s}=2$ [suggested by Atkinson (2000) and in this work for medium stresses, $q/q_u=0.5$]. To get the corresponding applied pressure, q, the Boussinesq solution [Eq. (3)] is applied to each G_{sec} value from the triaxial test, and the resulting K_{sec} value is multiplied by w_b . The results are shown in Figs. 16(c, f, and i) for the three case studies.

The three similarity approaches employed to predict pressuresettlement curves of the field tests for the three case study examples demonstrated reasonable results in the loading range considered. The absolute percentage errors of the predicted settlement against the measured value are given in Table 2 at $q/q_{u,\mathrm{pred}}=25\%$ and $q/q_{u,\mathrm{pred}}=50\%$. The classical similarity method provided remarkably good results for both the Bothkennar and Ballina sites. The best results were obtained with $c_q=0.8$, which showed a maximum error of 15%, increasing to 67% when including the Kinnegar site. Two-part similarity worked well for the Bothkennar site (less that 25% error). The remaining errors were higher and increased to over 100% for $c_{q,s}=2$, as suggested by Atkinson (2000) for stiffness similarity.

It is worth noting that as additional complexities, the pressure–settlement curve itself will be affected by the rate of loading, and behaviors such as creep or consolidation are not considered by the simplified approach of similarity presented herein.

The errors obtained from this approach should also be taken in context. Doherty et al. (2018a) conducted an international competition to predict the footing displacement of the two Ballina footing field tests. Out of the 50 submissions, they found that around 15% of submissions predicted the footing settlement to be within 50% of the measured value for $q/q_u=0.25$ and 22% for $q/q_u=0.5$. It is also worth noting that Doherty et al. (2018a) referred to the two field-tests as "almost identical foundations." Using the same method as previously, if Test 1 from the Ballina site is used to predict Test 2, percentage errors of 53% $(q/q_u=0.25)$ and 25% $(q/q_u=0.5)$ are obtained. This demonstrates the variability and uncertainty inherent in geotechnical design, even when a comprehensive site investigation is conducted. This also indicates that a simplified method such as similarity is well-suited for settlement estimation in routine design.

Table 2. Absolute percentage error of the similarity predictions in Fig. 16 at $q/q_u=0.25$ and 0.5

•		Bothkennar		Kinnegar		Ballina	
Method	Transformation factor	$q/q_u = 0.25$	$q/q_u=0.5$	$q/q_u = 0.25$	$q/q_u=0.5$	$q/q_u = 0.25$	$q/q_u=0.5$
Classical similarity	$\begin{array}{c} c_q = 0.5 \\ c_q = 0.8 \\ c_q \text{ from Eq. (4)} \end{array}$	33 6.8 81	45 12 49	79 67 36	79 66 34	47 15 42	42 7.9 54
Two-part similarity	$c_{q,p}$ from Eq. (22)	25	2.8	50	57	43	40
Stiffness similarity	$c_{q,s}$ from Eq. (29) $c_{q,s} = 2$	81 167	49 120	36 16	34 14	42 113	54 130

Summary and Conclusions

A simplified approach to obtain nonlinear pressure–settlement curves of vertically loaded, rigid, circular footings on clay has been presented. The "classical" similarity approach, originally suggested by Skempton (1951), relates the x-axis of a normalized stress–strain curve with that of a normalized pressure–settlement curve (Fig. 1). This transformation factor is defined in this work using a dimensionless linear-transformation factor c_q , defined by Eq. (1). In the original work, Skempton (1951) suggested that the stress–strain curve should be obtained from a routine soil element test (undrained triaxial compression) undertaken on a representative soil sample. Despite the theoretical importance and practical appeal of this simplified approach as well as its wide application in a range of geotechnical problems, limited investigation and validation exists in the literature. Motivated by this lack of knowledge, this paper initially investigated the classical similarity approach:

- Three related methods, an elastic stiffness approach based on the Boussinesq solution in Eq. (4) (Skempton 1951), the existing MSD method in Eq. (6) (Osman and Bolton 2005), and a novel cone model solution in Eq. (16), were reviewed and extended to derive c_q. A summary of c_q values obtained is shown in Fig. 6(a) and discussed.
- 2. The novel cone model solution demonstrates that c_q depends on the pressure applied to the foundation and gives a simple approach to determine this nonlinear function. The resulting c_q values are shown in Fig. 6(a).
- 3. It was found that for low stresses $(q/q_u < 0.05)$, the elasticity value of $c_q = 1.2$ [Eq. (4)] would be sufficient to stretch a stress-strain curve.
- 4. For higher stress levels, $q/q_u \approx 0.5$, (applicable in geotechnical engineering where safety factors of 2 to 3 are common), values in the range of $0.5 < c_q < 0.8$ are needed to compress a stress–strain curve [range from Fig. 6(a)].
- 5. For even higher stress regions, the c_q value appears to approach zero [Fig. 6(a)]. At this stress range, classical similarity is unlikely to be applicable, and more complex analysis considering soil plastic flow and failure should be sought. These results indicated that a higher applied footing pressure invariably results in increased strength mobilization and strain concentration in the area close to the footing, thus decreasing the characteristic dimension (c_qD).
- 6. For a rough footing, c_q was shown to be approximately 5% larger than that of a smooth footing, which indicates a marginally larger area of influence around the footing, increasing c_qD .

Contrary to the implied assumption in classical similarity, this paper has demonstrated that perfect similarity is unlikely for the problem at hand, and instead, c_q depends on load intensity. As an alternative, a two-part similarity procedure that consists of individual scaling factors on both the elastic, $c_{q,e}$, and plastic, $c_{q,p}$, portions of the stress–strain curve was investigated and applied to vertically loaded foundations for the first time. To this end:

- 7. The values $c_{q,e}$ and $c_{q,p}$ can be obtained from the Ramberg-Osgood model, applied for both the stress–strain curve and pressure–settlement curve [Eq. (22)] and calibrated with the aid of numerical analyses. According to Jakub (1977) and as further validated herein by comparison with numerical analyses, the elastic and plastic transformation factors obtained from the Ramberg-Osgood model can be generalized to other models as well.
- 8. The two-part similarity approach yielded $c_{q,e}=1.2$ and $c_{q,p}=0.5c_{q,e}$ ("Jakub-Roesset Method" section). Although these

- results remain dependent on footing roughness, the dependency on load intensity is reduced and can be applicable possibly as high as $q/q_u = 0.8$ (Fig. 13).
- 9. The values $c_{q,p}$ and $c_{q,p}$ can be converted into a single c_q value using classical similarity [Eq. (23)]. At low stress levels, c_q is naturally governed by $c_{q,e}$; however, the variation of c_q with increased applied loads is governed by the value of $c_{q,p}$. This paper recommends $c_{q,p} < 1$, which would suggest c_q decreases with an increasing applied load. Remarkably, this agrees with the classical similarity results but has the additional benefit of being controlled by a constant $c_{q,p}$.

As another alternative to the classical similarity method, Atkinson (2000) proposed a stiffness similarity approach that suggests similarity exists between the shear modulus reduction curve of a soil element with increasing strain $(G_s - \gamma)$ and the stiffness reduction curve of a surface foundation with increasing normalized settlement $(K_s - w_b/D)$. The transformation factor, $c_{q,s}$, and the application of this approach has been investigated in this paper. To this end:

- 10. Once again, perfect similarity does not exist, and the similarity factor, $c_{q,s}$ is dependent on the applied load intensity (Fig. 15).
- 11. For a perfectly plastic material, a value $c_{q,s} = 1.2$ can be analytically established [Eq. (29)]. This value is applicable at high stress ranges $(q/q_u = 1)$.
- 12. For lower applied stresses, values in the range $1.5 < c_{q,s} < 3$ would be applicable. This agrees with the $c_{q,s}$ suggested by Atkinson (2000) in the original work. However, it is evident that $c_{q,s}$ is dependent on the load intensity and, thus, a single value of $c_{q,s}$ is hard to determine. The stiffness similarity approach does not work well for low strains but, contrary to the other methods discussed, accuracy may improve with increased load intensity.

The results for all three approaches have been validated using numerical solutions in FLAC 2D using hyperbolic and tanh soil constitutive models and have been applied to three case study examples in Fig. 16.

It is important to mention that the similarity methods discussed are approximate solutions to obtain a nonlinear pressure–settlement curve of a vertically loaded circular footing. The transformation factors determined are (to varying extents) dependent on soil properties, applied load, and soil constitutive models. Although the methods are fundamentally approximate and accuracy in the results cannot be guaranteed, this should be considered in the context of the wider uncertainties present when predicting foundation settlements. These approaches enable simple, easy to understand solutions with clear assumptions, which can be easily obtained from standard site investigation tests.

Data Availability Statement

Some or all data, models, or code that support the findings of this study are available from the corresponding author upon reasonable request.

Acknowledgments

The authors would like to thank Dr. Ashraf Osman for his helpful advice and sharing his notes and code from his earlier work. The first author would like to thank the Engineering and Physical Sciences Research Council for their support (Grant No. EP/T517872/1).

References

- Agaiby, S. S., and S. M. Ahmed. 2022. "Assessing the nonlinear load-deformation relationships of vertically loaded shallow foundations on clays using the seismic piezocone testing." In *Proc.*, 20th Int. Conf. on Soil Mechanics and Geotechnical Engineering, 229–303. Sydney, Australia: Australian Geomechanics Society.
- Allman, M. A., and J. H. Atkinson. 1992. "Mechanical properties of reconstituted Bothkennar soil." *Géotechnique* 42 (2): 289–301. https://doi.org/10.1680/geot.1992.42.2.289.
- Atkinson, J. H. 2000. "Non-linear soil stiffness in routine design." Géotechnique 50 (5): 487–508. https://doi.org/10.1680/geot.2000.50.5.487.
- Bateman, A. H. 2025. "Simplified solutions for the non-linear response of axially and laterally loaded piles in clay." Ph.D. thesis, Dept. of Civil Engineering, Univ. of Bristol.
- Bateman, A. H., J. J. Crispin, and G. Mylonakis. 2022a. "A simplified analytical model for developing "t-z" curves for axially loaded piles." In *Proc.*, 20th Int. Conf. on Soil Mechanics and Geotechnical Engineering, 3211–3216. Sydney, Australia: Australian Geomechanics Society.
- Bateman, A. H., J. J. Crispin, P. J. Vardanega, and G. Mylonakis. 2022b. "Theoretical t-z curves for axially loaded piles." J. Geotech. Geoenviron. Eng. 148 (7): 04022052. https://doi.org/10.1061/(ASCE)GT.1943-5606.0002753.
- Bateman, A. H., G. Mylonakis, and J. J. Crispin. 2023. "Simplified analytical "m-θ" curves for predicting nonlinear lateral pile response." In *Proc.*, 9th Int. Offshore Site Investigation and Geotechnics Conf., 618–625. London: Society for Underwater Technology.
- Bishop, R. F., R. Hill, and N. F. Mott. 1945. "The theory of indentation and hardness tests." *Proc. Phys. Soc.* 57 (3): 147–159. https://doi.org/10.1088/0959-5309/57/3/301.
- Bolton, M. D., and W. Powrie. 1988. "Behaviour of diaphragm walls in clay prior to collapse." *Géotechnique* 38 (2): 167–189. https://doi.org/10.1680/geot.1988.38.2.167.
- Boussinesq, J. 1885. Applications des potentiels à l'étude de l'équilibre et mouvement des solides élastiques. Paris: Gauthier–Villard.
- Bowles, J. E. 1997. Foundation analysis and design. 5th ed. New York: McGraw-Hill.
- Bransby, M. F. 1999. "Selection of p–y curves for the design of single laterally loaded piles." *Int. J. Numer. Anal. Methods Geomech.* 23 (15): 1909–1926. https://doi.org/10.1002/(SICI)1096-9853(19991225)23:15<1909::AID-NAG26>3.0.CO;2-L.
- Brinch Hansen, J. 1970. An extended formula for bearing capacity. Danish Geotechnical Institute Bulletin No. 28. Copenhagen, Denmark: Danish Geotechnical Institute.
- Burland, J. B., F. G. Butler, and P. Dunican. 1966. "The behaviour and design of large diameter bored piles in stiff clay." In *Large bored piles*. London: Thomas Telford.
- Cox, A. D., G. Eason, and H. G. Hopkins. 1961. "Axially symmetric plastic deformations in soils." *Philos. Trans. R. Soc. London, Ser. A* 254 (1036): 1–45. https://doi.org/cf425k.
- Davies, R. O., and A. P. S. Selvadurai. 1996. Elasticity and geomechanics. Cambridge, UK: Cambridge University Press.
- Doherty, J. P., S. Gourvenec, and F. M. Gaone. 2018a. "Insights from a shallow foundation load-settlement prediction exercise." *Comput. Geotech.* 93: 269–279. https://doi.org/10.1016/j.compgeo.2017.05.009.
- Doherty, J. P., S. Gourvenec, F. M. Gaone, J. A. Pineda, R. Kelly, C. D. O'Loughlin, M. J. Cassidy, and S. W. Sloan. 2018b. "A novel web based application for storing, managing and sharing geotechnical data, illustrated using the national soft soil field testing facility in Ballina, Australia." *Comput. Geotech.* 93: 3–8. https://doi.org/10.1016 /j.compgeo.2017.05.007.
- Eason, G., and R. T. Shield. 1960. "The plastic indentation of a semi-infinite solid by a perfectly rough circular punch." *J. Appl. Math. Phys.* 11 (1): 33–43. https://doi.org/bpcw64.
- Elhakim, A. F. 2005. "Evaluation of shallow foundation displacements using soil small-strain stiffness." Ph.D. thesis, Dept. of Civil and Environmental Engineering, Georgia Institute of Technology.
- Foti, S., C. Lai, G. J. Rix, and C. Strobbia. 2015. Surface wave methods for near-surface site characterization. 1st ed. Boca Raton, FL: CRC Press.

- Fu, D., Y. Zhang, K. K. Aamodt, and Y. Yan. 2020. "A multi-spring model for monopile analysis in soft clays." *Mar. Struct.* 72 (Jul): 102768. https://doi.org/10.1016/j.marstruc.2020.102768.
- Gaone, F. M., S. Gourvenec, and J. P. Doherty. 2018. "Large-scale shallow foundation load tests on soft clay: At the National Field Testing Facility (NFTF), Ballina, NSW, Australia." *Comput. Geotech.* 93: 253–268. https://doi.org/10.1016/j.compgeo.2017.05.008.
- Gasparre, A. 2005. "Advanced laboratory characterisation of London clay." Ph.D. thesis, Dept. of Civil and Environmental Engineering, Imperial Collage London.
- Ghosh Dastider, A., P. Basu, and S. Chatterjee. 2021. "Numerical implementation of a stress-anisotropy model for bearing capacity analysis of circular footings in clays prone to destructuration." J. Geotech. Geoenviron. Eng. 147 (5): 04021019. https://doi.org/10.1061/(ASCE)GT .1943-5606.0002482.
- Gibson, R. E. 1950. "Correspondence on 'The bearing capacity of screw piles and screwcrete cylinders'." *J. Inst. Civ. Eng.* 34 (8): 374–386. https://doi.org/j98b.
- Gourvenec, S., M. Randolph, and O. Kingsnorth. 2006. "Undrained bearing capacity of square and rectangular footings." *Int. J. Geomech.* 6 (3): 147–157. https://doi.org/10.1061/(ASCE)1532-3641(2006)6:3(147).
- Hight, D. W., R. Böese, A. P. Butcher, C. R. I. Clayton, and P. R. Smith. 1992a. "Disturbance of the Bothkennar clay prior to laboratory testing." *Géotechnique* 42 (2): 199–217. https://doi.org/10.1680/geot.1992.42.2 .199.
- Hight, D. W., A. J. Bond, and J. D. Legge. 1992b. "Characterization of the Bothkennar clay: An overview." *Géotechnique* 42 (2): 303–347. https://doi.org/10.1680/geot.1992.42.2.303.
- Houlsby, G. T., and C. P. Wroth. 1984. "Calculation of stresses on shallow penetrometers and footings." In *Seabed mechanics*, edited by B. Denness, 107–112. Newcastle upon Tyne, UK: Springer.
- Ishlinsky, A. J. 1944. "The problem of plasticity with axial symmetry and Brinell's test." *J. Appl. Math. Mech.* 8: 201–224.
- Itasca Consulting Group. 2011. FLAC—Fast Lagrangian analysis of Continua in Two-Dimensions, Version 7. Minneapolis: Itasca Consulting Group.
- Jakub, M. 1977. "Nonlinear stiffness of foundations." M.Sc. thesis, School of Engineering, Massachusetts Institute of Technology.
- Jardine, R. J., B. M. Lehane, P. R. Smith, and P. A. Gildea. 1995. "Vertical loading experiments on rigid pad foundations at Bothkennar." *Géotech-nique* 45 (4): 573–597. https://doi.org/10.1680/geot.1995.45.4.573.
- Jeanjean, P., Y. Zhang, A. Zakeri, K. H. Andersen, R. Gilbert, and A. I. M. J. Senanayake. 2017. "A framework for monotonic P-Y curves in clays." In *Proc.*, 8th Int. Offshore Site Investigation and Geotechnics Conf., 108–141. London: Society for Underwater Technology. https:// doi.org/10.3723/OSIG17.108.
- Kagawa, T., and L. M. Kraft. 1981. "Lateral pile response during earth-quakes." *J. Geotech. Eng. Div.* 107 (12): 1713–1731. https://doi.org/10.1061/AJGEB6.0001222.
- Klar, A., and A. S. Osman. 2008. "Load–displacement solutions for piles and shallow foundations based on deformation fields and energy conservation." *Géotechnique* 58 (7): 581–589. https://doi.org/10.1680/geot .2008.58.7.581.
- Lai, Y., L. Wang, Y. Zhang, and Y. Hong. 2020. "Site-specific soil reaction model for monopiles in soft clay based on laboratory element stressstrain curves." *Ocean Eng.* 220 (Jan): 108437. https://doi.org/10.1016 /j.oceaneng.2020.108437.
- Lehane, B. M. 2003. "Vertically loaded shallow foundation on soft clayey silt." *Proc. Inst. Civ. Eng. Geotech. Eng.* 156 (1): 17–26. https://doi.org/10.1680/geng.2003.156.1.17.
- Martin, C. M., and M. F. Randolph. 2001. "Applications of the lower and upper bound theorems of plasticity to collapse of circular foundations." In *Computer methods and advances in geomechanics*, 1417–1428. Boca raton, FL: CRC Press.
- Matlock, H. 1970. "Correlations for design of laterally loaded piles in soft clay." In *Proc.*, 2nd Offshore Technology Conf., 557–588. Richardson, TX: OnePetro. https://doi.org/10.4043/1204-ms.
- McClelland, B., and J. A. Focht. 1956. "Soil modulus for laterally loaded piles." J. Soil Mech. Found. Div. 82 (4): 1081. https://doi.org/10.1061 /JSFEAQ.0000023.

- McMahon, B. T., S. K. Haigh, and M. D. Bolton. 2013. "Cavity expansion model for the bearing capacity and settlement of circular shallow foundations on clay." *Géotechnique* 63 (9): 746–752. https://doi.org/10 .1680/geot.12.P.061.
- McMahon, B. T., S. K. Haigh, and M. D. Bolton. 2014. "Bearing capacity and settlement of circular shallow foundations using a nonlinear constitutive relationship." *Can. Geotech. J.* 51 (9): 995–1003. https://doi .org/10.1139/cgj-2013-0275.
- Meyerhof, G. G. 1951. "The ultimate bearing capacity of foundations." *Géotechnique* 2 (4): 301–332. https://doi.org/10.1680/geot.1951.2.4 .301.
- Nash, D. F. T., G. C. Sills, and L. R. Davison. 1992. "One-dimensional consolidation testing of soft clay from Bothkennar." *Géotechnique* 42 (2): 241–256. https://doi.org/10.1680/geot.1992.42.2.241.
- Osman, A. S., and M. D. Bolton. 2004. "A new design method for retaining walls in clay." *Can. Geotech. J.* 41 (3): 451–466. https://doi.org/10.1139/t04-003.
- Osman, A. S., and M. D. Bolton. 2005. "Simple plasticity-based prediction of the undrained settlement of shallow circular foundations on clay." *Géotechnique* 55 (6): 435–447. https://doi.org/10.1680/geot.2005.55 .6.435.
- Osman, A. S., D. J. White, A. M. Britto, and M. D. Bolton. 2007. "Simple prediction of the undrained displacement of a circular surface foundation on non-linear soil." *Géotechnique* 57 (9): 729–737. https://doi.org/10.1680/geot.2007.57.9.729.
- Poulos, H. G., and E. H. Davis. 1974. Elastic solutions for soil and rock mechanics. New York: Wiley.
- Randolph, M. F., and C. P. Wroth. 1978. "Analysis of deformation of vertically loaded piles." *J. Geotech. Eng. Div.* 104 (12): 1465–1488. https://doi.org/10.1061/AJGEB6.0000729.
- Reese, L. C., and W. F. Van Impe. 2011. *Single piles and pile grounds under lateral loading*. 2nd ed. Boca Raton, FL: CRC Press.
- Salgado, R. 2022. The engineering of foundations, slopes and retaining structures. 2nd ed. Boca Raton, FL: CRC Press.
- Salgado, R., A. V. Lyamin, S. W. Sloan, and H. S. Yu. 2004. "Twoand three-dimensional bearing capacity of foundations in clay."

- Géotechnique 54 (5): 297–306. https://doi.org/10.1680/geot.2004.54.5.297.
- Salgado, R., J. K. Mitchell, and M. Jamiolkowski. 1997. "Cavity expansion and penetration resistance in sand." J. Geotech. Geoenviron. Eng. 123 (4): 344–354. https://doi.org/10.1061/(ASCE)1090-0241(1997) 123:4(344).
- Salgado, R., and M. Prezzi. 2007. "Computation of cavity expansion pressure and penetration resistance in sands." *Int. J. Geomech.* 7 (4): 251–265. https://doi.org/10.1061/(ASCE)1532-3641(2007)7:4(251).
- Seed, H. B., and L. C. Reese. 1957. "The action of soft clay along friction piles." Trans. ASCE 122 (1): 731–754. https://doi.org/10.1061/taceat .0007501.
- Shield, R. T. 1955. "On the plastic flow of metals under conditions of axial symmetry." Proc. R. Soc. London, Ser. A 233 (1193): 267–287. https:// doi.org/10.1098/rspa.1955.0262.
- Skempton, A. W. 1951. "The bearing capacity of clays." In Vol. 1 of Proc., Building Research Congress, 180–189. London: Building Research Station.
- Soga, K. 1994. "Mechanical behaviour and constitutive modelling of natural structured soils." Ph.D. thesis, Dept. of Engineering, Univ. of California at Berkeley.
- Spence, D. A. 1968. "Self similar solutions to adhesive contact problems with incremental loading." *Proc. R. Soc. London, Ser. A* 305 (1480): 55–80. https://doi.org/10.1098/rspa.1968.0105.
- Tani, K., and W. H. Craig. 1995. "Bearing capacity of circular foundations on soft clay of strength increasing with depth." Soils Found. 35 (4): 21–35. https://doi.org/10.3208/sandf.35.4_21.
- Wolf, J. P., and A. J. Deeks. 2004. Foundation vibration analysis: A strength-of-materials approach. Oxford, UK: Elsevier Science.
- Zhang, Y., and K. H. Andersen. 2017. "Scaling of lateral pile p-y response in clay from laboratory stress-strain curves." *Mar. Struct.* 53 (May): 124–135. https://doi.org/10.1016/j.marstruc.2017.02.002.
- Zhang, Y., and K. H. Andersen. 2019. "Soil reaction curves for monopiles in clay." Mar. Struct. 65 (May): 94–113. https://doi.org/10.1016/j .marstruc.2018.12.009.